THE JOURNAL OF PHYSICAL CHEMISTRY B
A JOURNAL OF THE AMERICAN CHEMICAL SOCIETY

pubs.acs.org/JPCB

Perspective

Dissecting Large-Scale Structural Transitions in Membrane Transporters Using Advanced Simulation Technologies

Shashank Pant,[†] Sepehr Dehghani-Ghahnaviyeh,[†] Noah Trebesch, Ali Rasouli, Tianle Chen, Karan Kapoor, Po-Chao Wen, and Emad Tajkhorshid*

Cite This: *J. Phys. Chem. B* 2025, 129, 3703−3719

Read Online

ACCESS | Metrics & More | Article Recommendations

ABSTRACT: Membrane transporters are integral membrane proteins that act as gatekeepers of the cell, controlling fundamental processes such as recruitment of nutrients and expulsion of waste material. At a basic level, transporters operate using the "alternating access model," in which transported substances are accessible from only one side of the membrane at a time. This model usually involves large-scale structural changes in the transporter, which often cannot be captured using unbiased, conventional molecular simulation techniques. In this article, we provide an overview of some of the major simulation techniques that have been applied to characterize the structural dynamics and energetics involved in the transition of membrane transporters between their functional states. After briefly introducing each technique, we discuss some of their advantages and limitations and provide some recent examples of their application to membrane transporters.

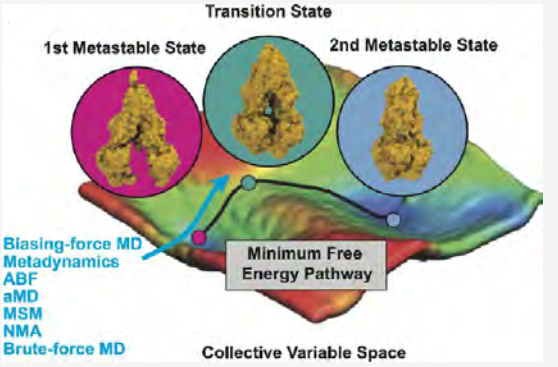

1. INTRODUCTION

As molecular machines, proteins rarely work as rigid bodies, and their function often relies on different modes and degrees of conformational changes. These conformational changes vary from local events such as side-chain or loop alterations, e.g., in response to enzyme substrates and products, to global events restructuring of the entire protein, e.g., to accomplish substrate movement in membrane transporters, or to interact with other biomolecules. As such, information from static structures is often insufficient in providing mechanistic details of the protein function. Molecular dynamics (MD) simulations, sometimes in conjunction with experimental single-molecule techniques, are commonly employed to fill this knowledge gap and provide dynamic representations of proteins and their conformational transitions among functional states. Current MD technologies limit conventional atomistic simulations of typical proteins from tens to hundreds of microseconds,[1] while functionally relevant conformational changes mostly happen on longer time scales. In order to study such relevant transitions, computational structural biologists often resort to enhanced sampling techniques that may be able to describe the transitions between different conformational states and even picture the free-energy landscape governing the process.[2] Several enhanced sampling methods have seen successfully applied in portraying significant biomolecular events, e.g., kinase activation,[3] gating of ion channels,[4] small-molecule and ion permeation,[5−7] transition between functional states in membrane transporters,[8−11] or describing protein−ligand[12−14] and protein−protein interactions.[15]

Similar to many other proteins, global conformational changes are at the heart of the function of membrane transporters. Membrane transporters are structurally highly diverse, and the nature of the conformational changes mediating substrate translocation in them can vary widely between different families[16,19,20] (Figure 1A). Like an ordinary enzyme, membrane transporters are featured with a binding site recognizing a specific substrate; however, their structures and mechanisms are significantly different in several ways. Notably, the "substrate" and the "product" of a membrane transporter are identical in chemistry but physically located in regions connected to the opposite sides of the membrane. The substrate's translocation across the membrane cannot be accomplished in one conformation, and the two half-pathways involved in the substrate movement which are located in the two halves of the protein form in different conformational states and connect the substrate binding site to either side of the membrane, a mechanism coined as the "alternating access

Received: January 6, 2025
Revised: March 4, 2025
Accepted: March 6, 2025
Published: March 18, 2025

https://doi.org/10.1021/acs.jpcb.5c00104
J. Phys. Chem. B 2025, 129, 3703−3719

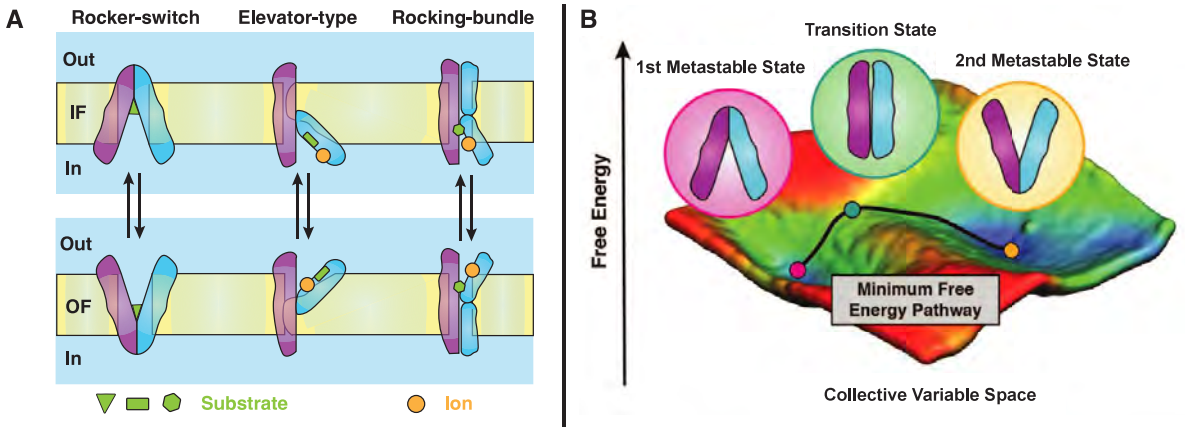

Figure 1. Schematic representation of major types of conformational changes[16] involved in the alternating access mechanisms[17,18] of membrane transporters and a representative free-energy landscape: (A) Major alternating-access modes of membrane transporters, with inward-facing (IF) and outward-facing (OF) states schematically shown in the top and bottom rows, respectively. From left to right the schematics show the rocker-switch, the elevator-type, and the rocking-bundle transport mechanisms. The membrane and solution are shown as yellow and blue media, respectively. The substrates are drawn as green shapes, while the cotransported ions, which usually drive the mechanism, as orange circles. (B) A representative free-energy landscape, describing different metastable and intermediate states of a membrane transporter during the transport cycle, calculated using a two-dimensional collective variable (CV) phase space. Colors show different free-energy values with blue and red representing low and high, respectively. The transporter's two domains are shown in purple and blue. Multiple conformational states of the transporters along the free-energy landscape are illustrated using pink, orange, and green circles. The black line represents the minimum free-energy pathway connecting the two functional end states.

mechanism",[17,18] even before any structural information for them was available.

With very few exceptions, e.g., the H^+/Cl^- antiport in ClC[21] or glucose permeation through GLUTs,[22] membrane transport by active transporters typically takes milliseconds to seconds, or even longer. For instance, a recent atomic force microscopy study of the glutamate transporter revealed that, in its fully bound state, it exhibits dwell times of several seconds in both the outward-facing (OF) and inward-facing (IF) conformations.[23] This slow "reaction rate" is almost always due to the transporter's global conformational change between its OF and the IF states, which forms the rate-limiting step of the reaction. During this slow step, the transporter needs to adjust its global conformation to coordinate the opening and closure of the two half-pathways in a coupled manner in response to factors such as substrate/cofactor binding/unbinding and/or the chemical reactions like ATP hydrolysis. Depending on the transporter structure, the coordination between different structural elements during transport can be either short- or long-range. Nevertheless, revealing the atomic details of the coupling mechanisms is essential to understand the transporter's function.

Studying the thermodynamic and kinetic properties of membrane transporters therefore cannot be accomplished by equilibrium MD simulations as a mainstream tool. Instead, they are better studied using enhanced sampling methods, which provide a more effective way to explore their global changes and the energy landscape associated with them (Figure 1B). This perspective provides an overview of some of the major enhanced-sampling methods that have been used in studying large-scale conformational changes of membrane transporters. We note that the limited space does not allow us to provide a comprehensive coverage of all the techniques used for this purpose or even all recent literature reported for the covered techniques. In particular, we are not able to cover techniques like transition path sampling[24,25] and shooting,[26] milestoning,[27] weighted ensemble,[28] and others.

The first described workflow takes advantage of user-defined biases and nonequilibrium simulations to construct an initial transition pathway in a user-defined collective variable (CV) space, which will be further refined and used for free-energy calculations. This workflow is followed by three highly related bias-based enhanced sampling techniques: metadynamics, adaptive biasing force (ABF), and accelerated MD (aMD). The application of biasing potentials in these techniques can be exploited to induce the structural transition and capture the energetics associated with it in different membrane transporters. As the next computational workflow, we describe the application of Markov State Models (MSMs) and adaptive sampling in capturing the energetics and kinetics of conformational transitions, which employ long time-scale unbiased MD simulations. This section is followed by using normal-mode analysis (NMA) as well as brute force MD whose application in some cases have been reported to capture structural transitions of membrane transporters between major functional states.

2. COMPUTATIONAL RECIPES TO STUDY LARGE-SCALE STRUCTURAL TRANSITIONS IN MEMBRANE TRANSPORTERS

Each section below will include brief description of a major method to study conformational transitions in membrane transporter, followed with brief discussion of its limitations and recent application example(s). We refer the reader to the cited papers for more technical details. As noted before, this perspective is not intended to be a comprehensive review of all methodologies and only uses a few major ones to showcase computational efforts in characterizing large-scale conformational changes in membrane transporters.

2.1. Applying Biases along User-Defined Collective Variables in MD. Because of the time scales involved in large-scale structural transitions of transporters, characterization of these transitions with MD usually requires biased simulations. In some MD-based methods, biases are defined and applied in an automatic way, but methods that apply biases explicitly defined by the user are more straightforward and more frequently used.

https://doi.org/10.1021/acs.jpcb.5c00104
J. Phys. Chem. B 2025, 129, 3703−3719

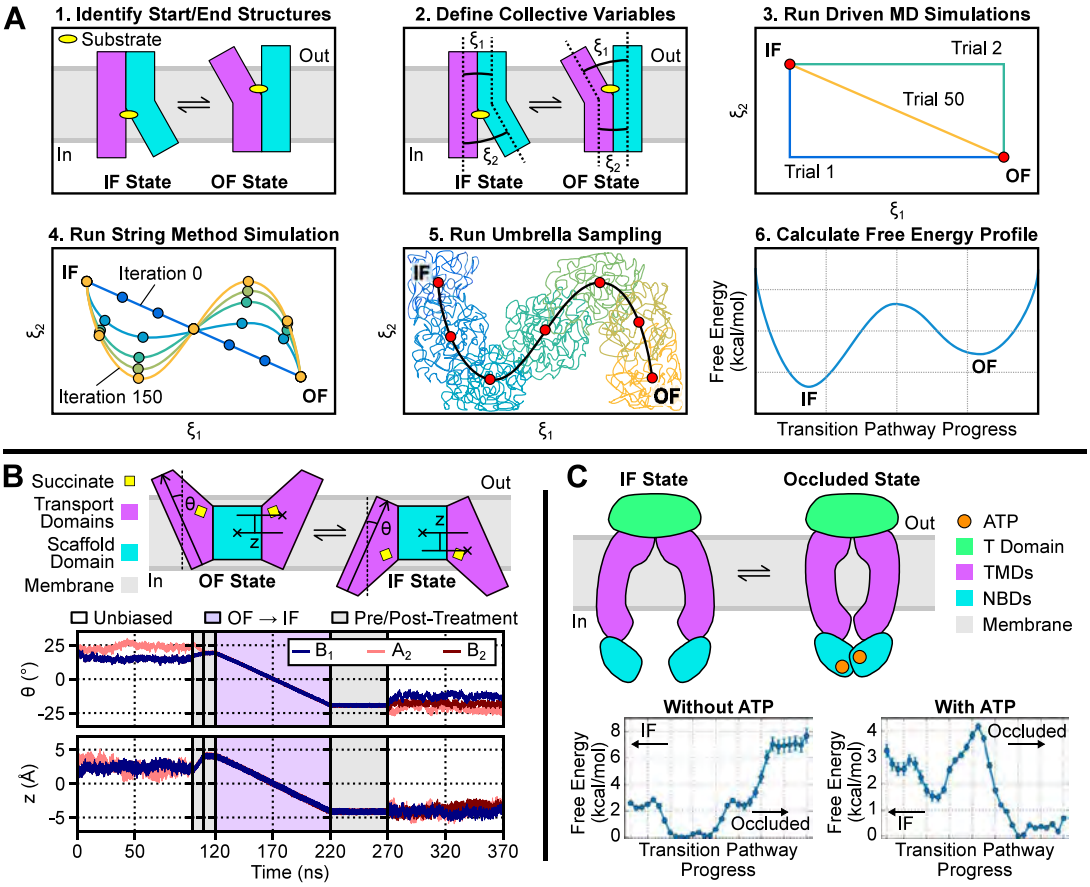

Figure 2. Overview and applications of a workflow of MD-based techniques that make use of user-defined biases to characterize large-scale structural transitions in transporters. (A) Schematic overview of the six stages of the workflow (see text for a detailed description of each step). (B) Application of the first three stages of the workflow to LaINDY, adapted from[31] (copyright 2020, Sauer et al. under the terms of the Creative Commons Attribution 4.0 International License). On top, schematic depictions of the OF and IF states of LaINDY along with schematic definitions of the CVs used to capture the major structural differences between the states are shown. On bottom, time series of the CVs for three protomer trials (B_1, A_2, and B_2) for the MD simulations in the study, including the main OF to IF driven MD simulation (purple background), are shown. (C) Application of the workflow to BhuUV-T (Reproduced from.[32] Copyright 2020 American Chemical Society). On top, schematic depictions of the IF and an OC state are shown. On bottom, free-energy profiles along a transition pathway between the states are shown. These profiles demonstrate that the OC state is the most stable state when ATP is bound, but the IF state becomes the most stable state once ATP unbinds.

Different MD-based methods with user-defined biases are used to explore various aspects of large-scale structural transitions in transporters. Here, we discuss one common workflow[8,29,30] that applies several of these methods in stages (Figure 2A).

In the first stage of this workflow, the start and end structures of a transition of interest within the transport cycle are identified. There are many transitions that can be investigated in a transport cycle, including the transition between the IF and OF states, the transition between an IF/OF state and an occluded (OC) state, and the transition between *apo* and bound IF/OF states. In some cases, both start and end structures have been characterized by high-resolution experimental methods, but in many others, they have to be refined (e.g., with MD flexible fitting, MDFF[33]) or modeled computationally (e.g., with homology modeling[34] or with inverted-repeat modeling[35]).

In the second stage, collective variables (CVs) are defined that capture the main differences between the start and end structures. CVs are mathematical functions defined on the spatial coordinates of a protein's atoms that are used to describe structural features of interest.[36] Common examples of CVs include the root-mean-square deviation (RMSD) of atomic positions in a protein, the center-of-mass (COM) distance between two domains of a protein, and the orientation of a helix or domain relative to another helix or domain within a protein.

In the third stage, driven MD is used to induce a transition between the start and end structures. In driven MD, harmonic biases are applied to the atoms used in the CV definitions and varied in a time-dependent manner to induce changes in that CV,[37] from the values associated with the start structure to the values associated with the end structure. Within this stage, several different transition pathways through the CV space may be tested, with biases applied to different CVs in different stages or at different rates, in an attempt to find a protocol that best describes the natural transition of the transporter. When studying transitions between IF and OF states, dozens of driven MD simulation trials are typically performed, and each transition is usually induced over ~20−200 ns, depending on the extent of the structural changes associated with the transition.[8,29−31,38,39]

In the fourth stage, a path refinement method called the string method is applied to relax the transition pathway generated by the driven MD simulations, a step that is essential to capture the full structural complexity of the natural transition pathway. In one implementation of this approach, called the string method with swarms of trajectories, a "swarm" of independent MD simulations is initiated at a series of points along the initial

https://doi.org/10.1021/acs.jpcb.5c00104
J. Phys. Chem. B 2025, 129, 3703−3719

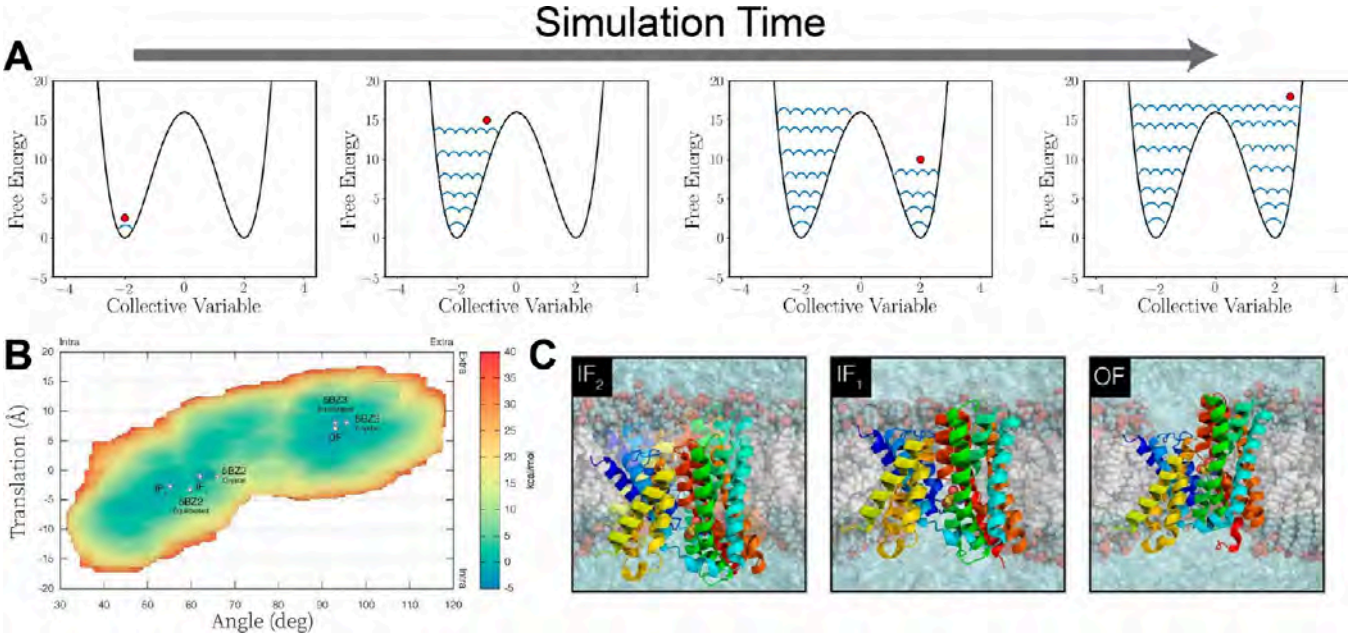

Figure 3. Overview and application example of metadynamics: (A) Schematic illustration of metadynamics, which can be described as "filling the free-energy wells with Gaussian-shaped biasing potentials". By continuously raising the effective energy of each well along predefined CVs, the method encourages the system to leave the energy wells and visit high-energy regions of the landscape. Once all the possible conformations along the defined CVs are sufficiently sampled, the system enters into a diffusive regime. (B) Example free energy surface derived from 2-CV metadynamics simulations of an antiporter (TtNapA). The estimated free energy landscape is calculated along the translation and orientation of transmembrane helices. The three main free-energy minima correspond to IF1, IF2, and OF state. (C) Representative conformations of TtNapA corresponding to the free-energy minima in B highlight the rocking-bundle motion for the alternating access mechanism in this transporter. Panels B and C are Reproduced from.[52] (Copyright 2020, National Academy of Sciences.).

transition pathway.[40] The simulations in each swarm are first driven to and restrained at their initiation points by applying harmonic biases to the previously defined CVs. Subsequently, the biases are released, allowing the simulations to drift freely for a short time.[40] The average drift of each swarm of simulations is then used to calculate new points along a new transition pathway through the CV space, and the above procedure is repeated until the transition pathway converges.[40] In typical applications of the string method with swarms of trajectories to large-scale conformational transitions of transporters, ∼500−1500 independent MD simulations are run for ∼1−10 ns each.[8,41,42]

Finally, in the fifth stage, umbrella sampling (US)[43,44] is applied to enhance sampling along the relaxed transition pathway, which enables techniques like the weighted histogram analysis method (WHAM)[45] or multistate Bennett acceptance ratio (MBAR)[46] to be used to estimate free energy profiles along the transition pathway. In a US simulation, a series of MD simulations (i.e., "replicas") are initiated at points along the transition pathway.[44] The replicas are restrained to their initiation points by applying harmonic restraints to the previously defined CVs, and the replicas are run until the free energy profile along the transition pathway converges.[44] In the so-called replica-exchange variant of US (REUS), designed to improve the smoothness of the converged free energy profile, the harmonic restraints applied to pairs of replicas are swapped (or "exchanged") throughout the simulation when certain conditions are met.[29,47] When characterizing transitions between IF and OF states, US or REUS simulations will typically include ∼20−200 replicas each run for ∼20−100 ns.[8,29,30,32,42,48]

By applying this workflow to investigate a large-scale structural transition in a transporter, the user obtains an atomic-resolution trajectory and free-energy profile along a relaxed transition pathway. This level of characterization is highly detailed and valuable, but it is not comprehensive, as it notably lacks any information regarding the kinetics associated with the transition. Additionally, while all simulations are performed with the transporter solvated and embedded in a membrane, the atomic-resolution trajectory is generally limited to the transporter itself, as the positions of lipid and water molecules are generally not required to be continuous along the transition pathway in string method and US simulations.

Among the methods used to characterize large-scale structural transitions in transporters, the use of CVs in this workflow is an important distinguishing feature. Proper CVs must be selected and defined with great care such that they accurately, specifically, and comprehensively capture the structural differences between a pair of structures, as poor CVs will result in correspondingly poor structural and thermodynamic characterization of the transition. Using CVs focuses the large amounts of computation required by this workflow on the specific transition defined by the user. A drawback of this focus is that automatic, unsupervised exploration of the transporter's conformational space is not possible within this workflow.

Beyond the selection and definition of CVs, there are several other empirical components that pervade the rest of this workflow. Such components include, for example, the strength of the biases applied to the CVs during each stage of the workflow, the choice of the pathway through the CV space during the driven MD simulation, the length of the driven MD simulation, the number of swarms in the string method with swarms of trajectories simulation, the number of simulations to run per swarm, the simulation length of each iteration of the string method, and the number of points along the transition

https://doi.org/10.1021/acs.jpcb.5c00104
J. Phys. Chem. B 2025, 129, 3703−3719

pathway where replica simulations are initiated during the US simulation. Each of these empirical components of the overall workflow can and should be guided by quantitative analysis of the resulting simulations in each stage of the workflow, but this necessitates extensive user supervision and trial-and-error and is significantly aided by substantial user experience and the development and application of general "rules of thumb."

2.1.1. Application Example I: Inducing Transitions between Functional States of a Metabolite Transporter. There are many recent examples in which different combinations of stages of the MD-based workflow described above have been used to characterize large-scale structural transitions in transporters. One such study[31] applied the first three stages of the workflow to LaINDY, an elevator-type antiporter that is a bacterial homologue of a human metabolite transporter. In this work, an X-ray crystal structure captured the OF state of LaINDY, and the IF state was modeled using the theory of inverted repeats. CVs were defined to capture the large-scale rigid-body translation and rotation of LaINDY's transport domains relative to its scaffold domain, and driven MD simulations using these CVs were run to induce the OF to IF transition (Figure 2B), providing detailed mechanistic insights into the transition that were often complemented by experimental results. In two other recent exemplary studies, the first three stages of the workflow were similarly applied to the transporters EmrE,[38] a rocker switch-type antiporter that is an archetypal member of the small multidrug resistance transporter family, and Mhp1,[39] a rocking bundle-type symporter that is a member of the LeuT-fold transporter superfamily.

2.1.2. Application Example II: Generating Free-Energy Profiles along Relaxed Transition Pathways. Another noteworthy recent study[32] applied the latter stages of the workflow to BhuUV-T, an ATP-binding cassette (ABC) heme importer from pathogenic bacteria. In this study, a driven MD simulation induced a transition from a model of an OC state to the IF state using overall RMSD of the protein as the CV. This simulation was repeated both in the presence and absence of bound ATP, the energy source for the transition. These initial transitions were then relaxed using the string method, and free-energy profiles along the pathways were calculated using US followed by MBAR. These profiles validated the model of the OC state and revealed the role that ATP plays in inducing the transition (Figure 2C). In three other exemplary studies, the latter stages of the workflow were similarly applied to SERCA, an ABC-type Ca^{2+} pump of the sarcoplasmic reticulum,[41] AcrB, a multidrug exporter,[48] and rGLUT5, a rocker switch-type glucose uniporter.[42]

2.2. Metadynamics. Metadynamics is another enhanced sampling algorithm that uses biases along predefined CVs to capture thermodynamics and kinetics properties of a molecular process.[49−51] Similar to many other enhanced sampling methods, this approach requires a low-dimensional space (provided by CVs) that can effectively describe the process of interest. A history-dependent bias is then constructed, in the form of Gaussian-shaped potentials along the defined CVs that discourage the system from revisiting previously sampled regions of the space, resulting in an efficient exploration of the full surface (Figure 3A).

In the original formulation of the method, one would not know when to stop the simulation, and the free energy would not converge to a certain value, leading to errors. While decreasing the frequency of adding Gaussians would reduce this error, it would add to the simulation time needed to fill the energy wells. Furthermore, once all the energy wells are filled, continuing the simulation carries the risk of driving the system into physically meaningless regions of the phase space. This problem was later ameliorated by employing approaches like well- and parallel-tempered metadynamics, which are currently the most commonly used variants of the method. In well-tempered variant the height of the Gaussians is scaled with the simulation time.[51] Parallel-tempered metadynamics, on the other hand, works by running multiple copies of a system at different temperatures while also applying the metadynamics biasing potential on each replica.[53]

The deposition of history-dependent biases counter the high-energy regions in the underlying free-energy landscape, in an iterative manner, encouraging the system to escape the energy minima via lowest energy pathways. This property not only renders metadynamics an attractive approach to accelerate rare events but also to calculate the free energy and kinetic rate constants associated with the process. However, it is important to note that calculating kinetic rate constants from this approach is not trivial and can only be calculated when no-bias is deposited in the transition states.[54]

Although metadynamics is a robust and relatively easy-to-use method, its efficiency scales poorly with the number of CVs and, in practice, is limited to three CVs. To some extent, the convergence and accuracy of metadynamics results depend on the choice of input parameters, such as the magnitude of the biasing potential and its deposition frequency. Similar to the method described in the previous section, these parameters are fairly empirical, and there is no straightforward way to choose them *a priori*.

Metadynamics has been used in studying membrane transporters rather extensively.[55−58] Here we highlight two such applications and briefly discuss their results.

2.2.1. Application Example I: Formation of Channel-Like Intermediates in a Neurotransmitter Transporter. In a recent study[11] well-tempered metadynamics with system-specific CVs was utilized to drive conformational transitions in the human excitatory amino acid transporter 1 (EAAT1). EAAT1 plays a critical role in glutamate reuptake from the synapse and is also involved in Cl^- ion conductance,[11] which is critical for its physiological function. The study used metadynamics to allow the system to overcome energy barriers that would otherwise be inaccessible in standard MD simulations and to explore the free-energy landscape underlying structural changes of EAAT1. By carefully selecting CVs that capture conformational changes of EAAT1, the authors were able to enhance sampling of rare states within hundreds of nanoseconds of metadynamics runs, including capturing the structure of the channel-like, Cl^--conducting intermediates. By combining well-tempered metadynamics with μs-long US the authors showed the mechanism of uncoupled translocation of Cl^- ions through the transporter's pore in a channel-like conformation. The calculations enabled the sampling of an intermediate conformation that occurs during the transport cycle of this human neurotransmitter transporter. Additionally, free-energy calculations for ion movement through the captured conformations revealed the presence of hydrophobic gates that regulate access to the aqueous pathway.

2.2.2. Application Example II: Studying Conformational Transitions in a Cation/Proton Antiporter. Another recent study[52] employed well-tempered metadynamics to capture conformational transitions in TtNapA, a cation/proton antiporter from *Thermus thermophilus* (Figure 3B,C). History-dependent biasing potentials were deposited simultaneously

https://doi.org/10.1021/acs.jpcb.5c00104
J. Phys. Chem. B 2025, 129, 3703−3719

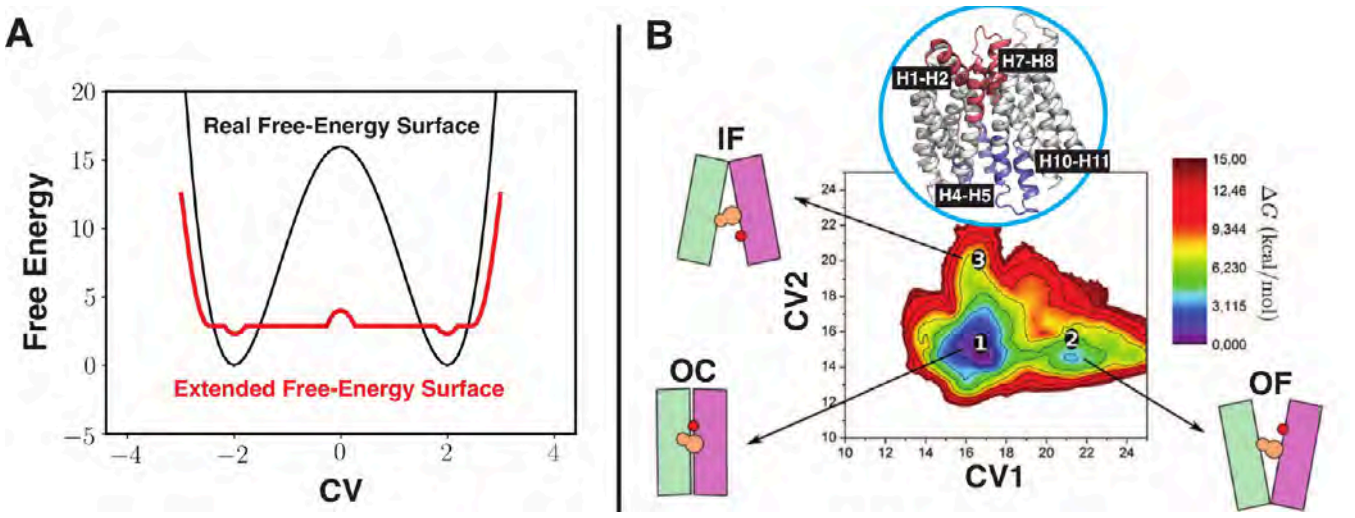

Figure 4. Overview and application of ABF: A) Schematic representation of ABF application to a one-dimensional PMF. The black line represents the unbiased PMF, while the red line shows the effective PMF that the system feels after the application of ABF. ABF biases the system in the direction of a CV, resulting in a flattened PMF and, therefore, enhances the sampling. B) The free-energy landscape, reconstructed from an ABF simulation, for $PepT_{st}$ in the proton- and substrate-bound state. CV1 represents the COM distance between H1−H2 and H7−H8 (red in the molecular view), whereas CV2 is the COM distance between H4−H5 and H10−H11 (green). (Reproduced from.[64] Copyright 2019, American Chemical Society.) In the schematics, the protein's two bundles are shown in green and magenta cylinders, respectively, along with the proton and substrate in red and orange circles. States 1−3 in the free-energy landscape correspond to OC, OF, and IF conformational states, respectively. The OC represents the global minimum while the OF and IF states correspond to metastable states under the proton- and substrate-bound conditions.

along two CVs defined by the translational and orientational motions of a protein domain, as well as those just along the orientational space. The simulations were able to capture the alternate conformation, in support of a rocking-bundle mechanism as the mode of the conformational change. Similarly, metadynamics has also been used to capture the unknown OF conformation of EcNhA, a bacterial cation/proton antiporter.[52]

2.3. Adaptive Biasing Force. Adaptive biasing force (ABF) is another enhanced sampling technique to capture rare events and associated free-energy landscape in a CV space.[59,60] The free-energy changes along a certain CV (or in a space of multiple CVs) can be interpreted as a potential generated from an average force acting on the system along the same direction in the phase space, also known as potential of mean force (PMF).[61,62] ABF takes advantage of this concept and tries to flatten the underlying free-energy landscape and overcome high-energy barriers in an adaptive fashion without any prior knowledge of the landscape.[63] During the course of an enhanced sampling simulation with ABF, the algorithm calculates and records the instantaneous force acting along each CV. The time average of the recorded forces is a good estimate of the mean force, that is, the negative of the PMF gradient. The algorithm then adds a biasing force to the system, the value and sign of which are equal and opposite to the estimated mean force, respectively, resulting in the molecular system experiencing an effectively flattened PMF, and therefore, accelerating the sampling along the CVs (Figure 4A).

Similar to other biasing protocols, one of the main challenges faced by ABF simulations is the convergence of the free energy landscape, especially in complex systems when more than one CV is required. Since ABF relies on applying a biasing force along chosen CVs to enhance sampling, it can struggle with slow convergence and incomplete exploration of the conformational space, particularly when the process is associated with high-energy barriers or rugged landscapes. To alleviate this problem, methods like the multiwalker ABF (MW-ABF) have been devised,[65,66] in which multiple parallel walkers are used to better explore the phase space. Each walker is updated independently, but their biasing potentials are averaged over time, ensuring that the system samples the conformational space more efficiently. By distributing the sampling across independent walkers, MW-ABF reduces the likelihood of being trapped in local minima and thereby improves the convergence of the resulting free-energy profile.

2.3.1. Application Examples. The ABF method has been extensively used for studying the energetics of different biochemical phenomena, e.g., bilayer permeability,[67] water permeation through a peptide nanotube,[68] and peptide folding.[69] Recently, ABF was employed to shed light on the conformational transition and free-energy landscape of $PepT_{st}$, a bacterial transporter from the proton-coupled peptide transporter (POT) family.[64] $PepT_{st}$ consists of two helical bundles, N- and C-terminal, composed of transmembrane (TM) helices H1−H6 and H7−H12, respectively. Structures of $PepT_{st}$ have shown two binding cavities located at the intracellular and extracellular sides of its lumen, respectively, which participate in binding and translocation of the substrate. The intracellular binding cavity is formed by the H4−H5 and H10−H11 helices, whereas, the extracellular binding cavity is constructed by the H1−H2 and H7−H8 helices.

The alternating access model[17,18] here follows the rocker-switch model and includes IF, OC, and OF conformational states. Considering the structural information, a 2-dimensional CV space was constructed to study the conformational transition and free-energy landscape by ABF: one CV described the COM distance between the tips of H1−H2 and H7−H8, and the other the COM distance between the tips of H4−H5 and H10−H11. The tips were defined as the first 10 C_α atoms of each helix. The aforementioned CV space was then used to apply the bias using the ABF algorithm, to induce the conformational transition of $PepT_{st}$. The effects of proton coupling and substrate binding on the free-energy landscape were also investigated,

https://doi.org/10.1021/acs.jpcb.5c00104
J. Phys. Chem. B 2025, 129, 3703−3719

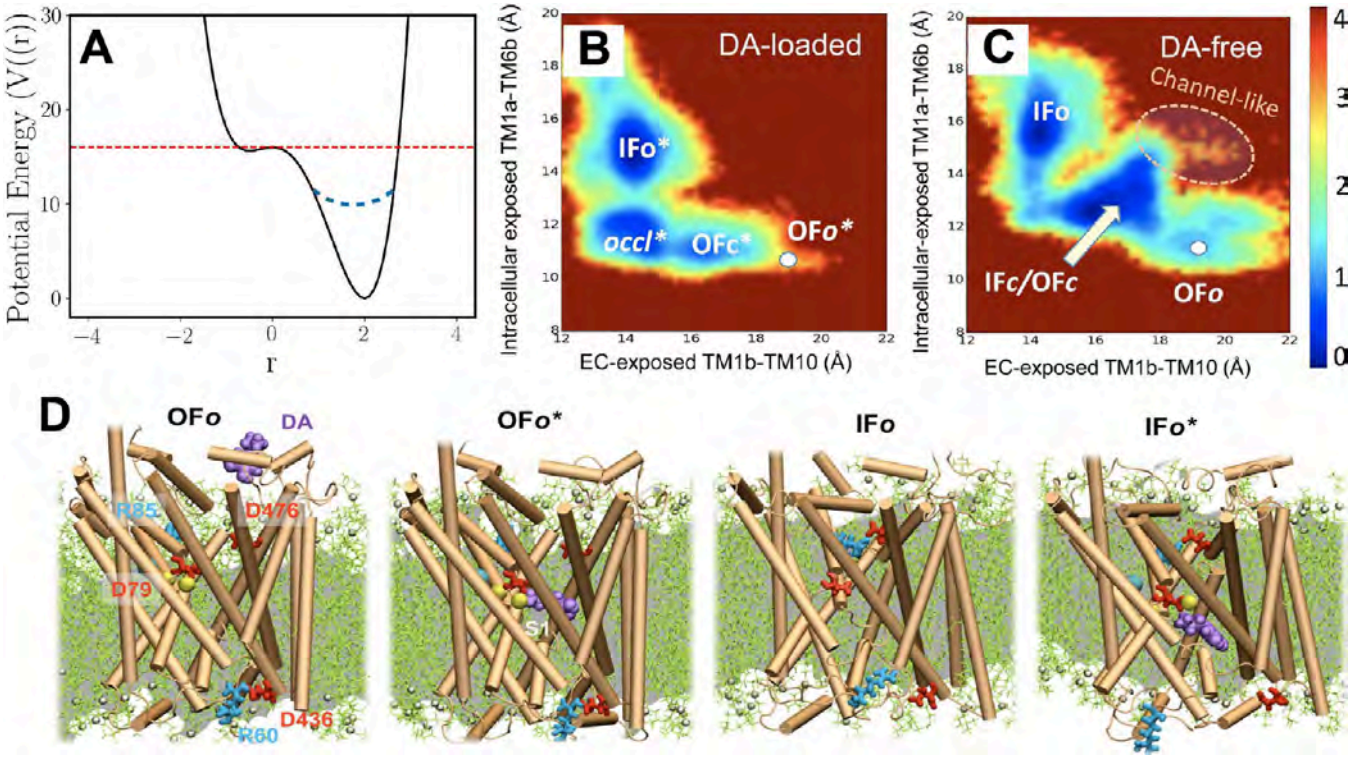

Figure 5. Overview and applications of aMD: (A) Schematic representation of a regular potential energy term (solid black line), the boost potential deposited in the energy minima (dashed blue line), and the threshold for boost energy (dashed red line) in an aMD simulation. If set up properly, the energy basins are altered by the deposition of boost potentials, while the transition states are left unaltered. (B, C) Conformational energy landscape of hDAT in substrate-loaded and substrate-free states calculated by aMD simulations. The regions colored in blue are the free-energy minima, while the regions in brown were not sampled in the simulations. In both states multiple conformations, including intermediate channel-like conformations, were captured in these simulations. (D) Four major conformations captured during the transport cycle of hDAT: OF-open with the substrate (DA: purple, space-filling) away from the binding site (OF_o), OF-open with the substrate bound in its binding site (OF_o*), IF-open without the substrate (IF_o), and IF-open with the bound substrate (IF_o*). The translocated substrate and ion, as well as critical residues are shown with different colors. Panels B-D are reproduced from.[70] (Copyright 2020, American Chemical Society.)

concluding that the OF state was stable only when the transporter was simultaneously bound to the proton and the substrate. For this fully bound state, the OC conformation was the most stable state (global minimum), and the IF and OF conformations represented metastable states.

2.4. Accelerated Molecular Dynamics. The general idea behind accelerated MD (aMD) is the deposition of non-negative boost potentials to decrease the energy barriers of regular energy terms and thus accelerate the transitions between minimum-energy conformations.

In aMD, a potential energy function is defined such that when the potential energy originated from the force field is below a certain threshold, the simulations are performed on a modified potential energy surface (Figure 5A). Otherwise, the simulations use unmodified potential energy terms. Therefore, by construction the potential energy near the minima are raised and those near the transitions are left unaltered. Unlike the previously mentioned enhanced sampling methods, aMD does not require predefined CVs, an aspect that can be advantageous for studying complex molecular systems without *a priori* knowledge. In practice, the choice of boost and the cutoff potentials need to be properly done because low boost potentials will result in an ineffective potential and too high boost potentials will result in noisy statistics.

Although aMD has been successfully applied to capture various biomolecular processes, the boost potentials applied in aMD are typically on the order of tens of kcal/mol (or more), which creates problems for accurately reweighting aMD trajectories and recovering the underlying free-energy surfaces, especially for large biomolecular systems.[71,72] This problem has been alleviated, in part, by the use of Gaussian aMD (GaMD),[73] which uses near Gaussian-shaped boost potentials.

2.4.1. Application Examples. The past few years have witnessed many studies employing aMD and GaMD to investigate various biophysical processes, for example, conformational dynamics of GPCRs,[74] peptide binding,[75] and ligand-protein interactions.[76] Here we briefly describe a recent application of aMD to study large-scale conformational transitions in a membrane transporter. In a recent study,[70] hundreds of nanosecond-long aMD was employed in a multiple replicas to study global conformational transitions between the OF and IF states of hDAT, the human dopamine transporter that regulates dopaminergic signaling by removing dopamine (DA) from the synapse. Interestingly, without a predefined target conformation, aMD was able to capture local and global structural transitions of hDAT (Figure 5B,C). The simulations were able to resolve the mechanism of DA translocation and accompanying protein structural transformations over a complete transport cycle (Figure 5D). notably, due to the extensive sampling of the conformational transitions, these simulations were also able to capture a channel-like, intermediate conformation in which a continuous aqueous pathway connecting extracellular and intracellular milieu was formed.

https://doi.org/10.1021/acs.jpcb.5c00104
J. Phys. Chem. B 2025, 129, 3703−3719

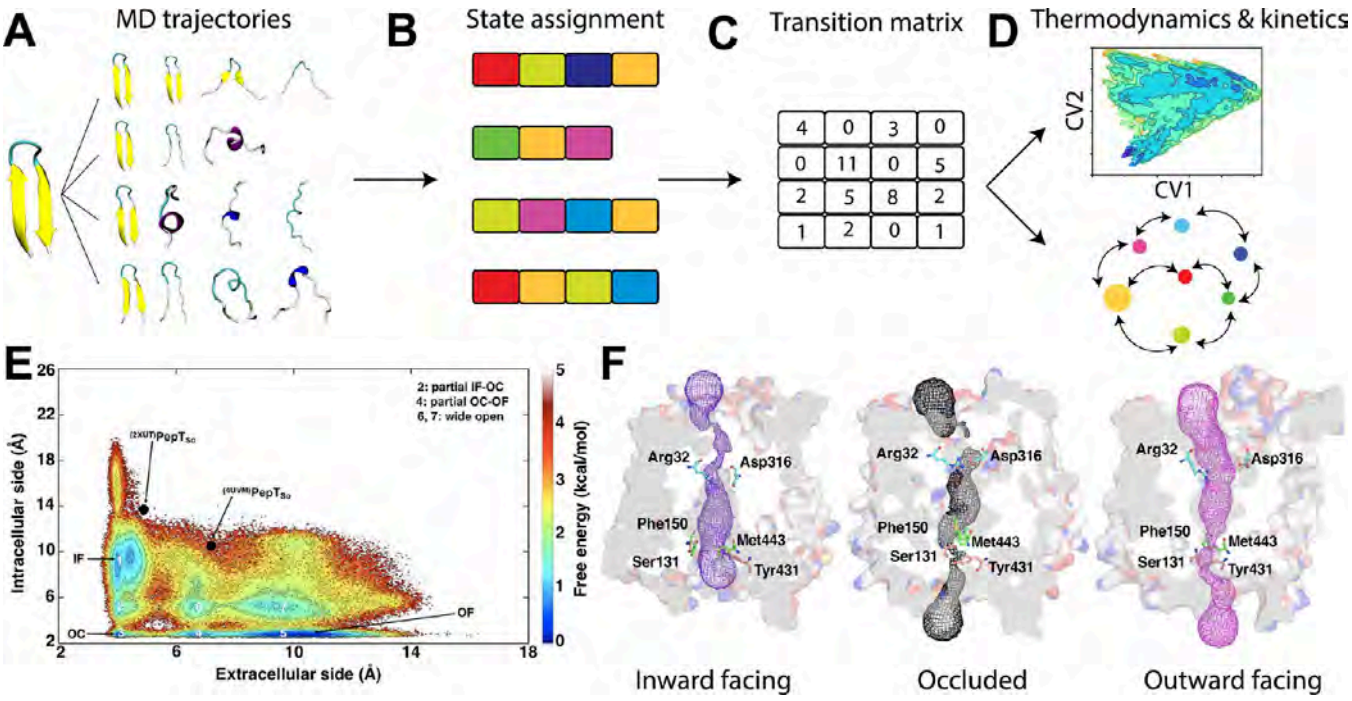

Figure 6. Overview and applications of Markov State Modeling: (A) Multiple independent adaptive MD trajectories of a biomolecular system are first performed in an iterative and exploratory manner.[81] (B) A discrete state decomposition of the trajectories, in which multiple states (green, blue, purple, and pink) are defined. (C) The transition probability matrix records how many times the system transitions between the defined states. (D) Calculated free-energy landscape in a low-dimensional space and corresponding kinetic rates. (E) Conformational energy landscape of $PepT_{So}$, projected on a 2-dimensional space (Reprinted from.[82] Copyright 2020, American Chemical Society). Multiple stable and metastable conformational states were captured during the simulations. (F) Distinct conformational states of $PepT_{So}$, namely IF, OC, and OF.

2.5. Markov State Modeling. Markov state models (MSMs) use a master-equation framework, typically constructed from an extensive set of adaptive MD trajectories (Figure 6A). They describe a detailed kinetic picture of the transitions between the states of the molecular system which are assumed to be in dynamic equilibrium.[77] In MSM, one constructs an $n \times n$ matrix, referred to as the "transition probability matrix", where n is the number of states.[78,79] The population of the states is determined by employing an adaptive MD simulation scheme,[80] where the dynamical progression of the system is tracked by determining which state it occupies at different lag times (τ) (Figure 6B).

In these simulations, it is important to make sure that the process is Markovian, namely, that the transition between any two states does not depend on where the system was before, i.e., its history. The elements of the transition probability matrix correspond to the transition probabilities between the states after lag time τ, with the diagonal ones corresponding to self-transitions (Figure 6C). The population of each state can provide insights into the energy landscape, and transition probabilities can be utilized for calculating kinetic properties (Figure 6D). Thus, the ultimate goal in MSM is to select an optimal number of n states and an optimal lag time that can best characterize the dynamics of the system and provide molecular insight. The method is available to the scientific community as a set of Python-based scripts published in MSMBuilder[83] and PyEMMA[84] software packages.

With well constructed MSMs, the user obtains an atomic-level description of the partitioned states for the simulated system, as well as their underlying energetic and kinetic landscape. A main difficulty in constructing accurate MSMs is the trade-off between approximation and the statistical errors. While a proper partitioning of the low-dimensional space will lead to small approximation errors, low-quality or insufficient MD data may lead to a significant increase in the error. Apart from this, a major question in the field is how to accurately define a low-dimensional space that would provide an accurate description of the eigenfunctions of the Markov operator.

2.5.1. Application Examples. Many recent studies have employed MSM to characterize conformational dynamics of GPCRs,[85] tumor proteins,[86] kinases,[87] ligand-protein interactions,[88] and transporters.[89−93] Here we briefly discuss the results of a two recent applications of the method to membrane transporters. Multi-μs MD simulations in conjunction with MSM highlighted a significant contrast between the conformational dynamics of SWEET and SemiSWEET transporters, a family of sugar transporters which play an important role in cellular exchange of carbon sources.[94] As compared to the *apo* conformation, the substrate-bound SWEET transporter showed a reduced free-energy barrier to transition between the OF and IF states, while no such reduction in the free-energy barrier was observed for SemiSWEET transporters.[94] Interestingly, these simulations were also able to capture a wide conformational heterogeneity in the SWEET transporter, which might allow it to accommodate various substrate conformations.

In another study,[82] MSM combined with transition path theory (TPT) provided thermodynamic and kinetic information on complex structural changes in $PepT_{So}$, a proton-coupled bacterial symporter. The simulations could capture multiple biochemically relevant intermediate states. The reweighted free-energy landscape revealed stable and metastable regions corresponding to different functional states of the protein (Figure 6E,F). Furthermore, TPT was applied to capture the most probable pathway for the structural transitions, which

https://doi.org/10.1021/acs.jpcb.5c00104
J. Phys. Chem. B 2025, 129, 3703−3719

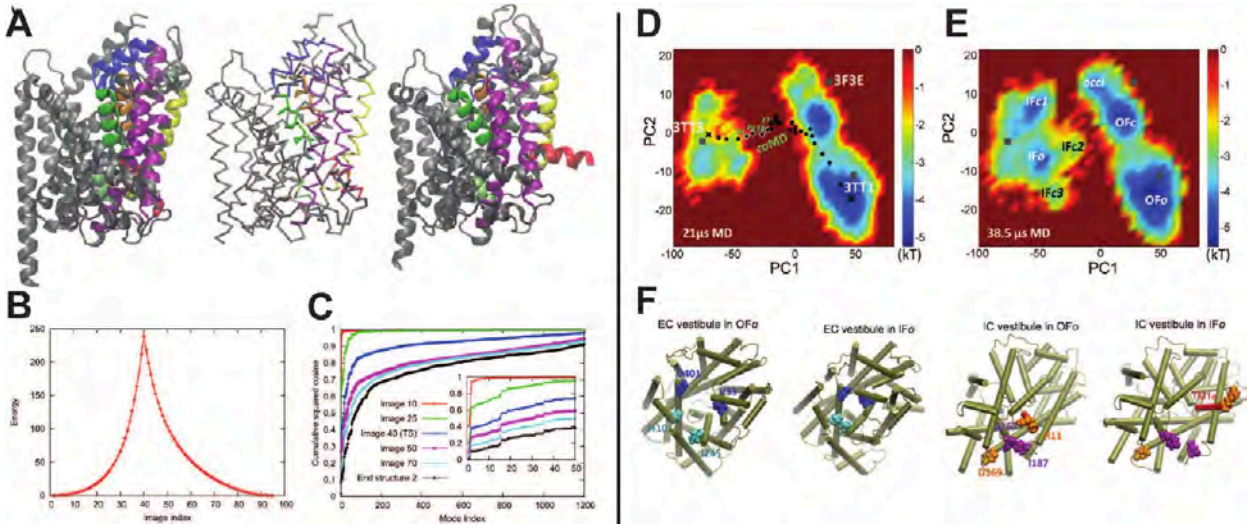

Figure 7. Application examples of normal-mode analysis: (A) Conformational transition between the OF, IF, and OC states of LeuT described by NMA. The scaffold domain (gray) does not undergo large-scale conformational changes. The transition state produced by 2s-ANM is depicted in the central figure. (B) The energy of the system along the $OF_{occluded} \rightarrow IF_{open}$ conformational transition. (C) Normal mode projections of LeuT conformers along the transition pathway show that, at first, only a few normal modes are needed to describe conformational changes. As the transition progresses, more normal modes are required to capture the complex changes from the reference (OF occluded) state. Panels A-C are Reproduced from ref[102] Available under a CC-BY 4.0 license. Copyright Das et al. (D) The energy landscape of LeuT's transition obtained from conventional MD simulations shows two main energy minima, representing the IF and OF states. However, the area between these two states could not be explored. On-pathway conformations generated with collective MD, a hybrid approach that simulates conformational dynamics of the system by biasing it along normal modes predicted by ANM, are shown in black dots. (E) Energy landscape for LeuT's transition obtained by combining conventional MD with the simulations starting from collective MD conformers. (F) Multiple LeuT structures with varying degrees of extracellular and intracellular openings are shown. Panels E-F are reproduced from,[103] with the permission of AIP Publishing).

converts the system from the OF state to the IF state via an OC intermediate. These simulations were also able to characterize critical residues at the extra- and intracellular gates that control the functional state of $PepT_{So}$.

2.6. Normal Mode Analysis. A protein can undergo a broad range of thermal fluctuations at room (or body) temperature and sample an ensemble of conformations. Regular MD, when performed long enough and with accurate force fields, should be able to capture all of these conformations and the deformations connecting them.[95] While most of the deformations represent thermal noise and are not relevant functionally, a number of them can collectively capture the motion of the protein during its function. Normal mode analysis (NMA) is a technique allowing one to study such deformations (normal modes) in a protein, or other macromolecular system.[96] A select group of normal modes that are deemed functionally relevant can then be used to bias the motion of the protein and explore its functional dynamics.[97,98]

While a full representation can in principle be used for this purpose, the technique is often used with coarse-grained representations of a protein,[99] where the molecular structure is simplified as, e.g., a single or multiple interaction site per residue.[97,98,100] For example, the protein can be modeled as a network of neighboring sites, typically represented by the positions of the Cα atoms, which are connected by simple springs according to a proximity criterion. The simplest NMA models assume the springs to have uniform force constants for all connections. Using the starting structure as a reference point, for which the potential energy of the network is defined to be minimum, the normal modes are then calculated by diagonalizing the Hessian matrix, a $3N \times 3N$ matrix that encodes the second derivatives of the potential energy, where N is the number of particles in the system.

Normal modes can be calculated in two different spaces: (1) in the internal coordinate space, or (2) in the Cartesian coordinate space.[101] While using Cartesian coordinates is easier to set up, calculation of normal modes in internal coordinates simplifies the analysis due to their more convenient physical interpretation. The normal modes represent the different molecular deformations away from the global minimum-energy configuration. The lowest-frequency modes require the least energy for (the same degree of) deformation, representing the softest and often most functionally relevant modes. However, it is important to note that many of them often correspond to "localized" structural deformations such as loop motions rather than "collective" (global) movements of the protein. Therefore, careful inspection is needed to determine whether a mode engages a large portion of the protein structure and thus reflects global structural rearrangements, as only those modes are of interest when trying to describe, e.g., global structural transitions in a membrane transporter.

Normal mode calculations only require the position of the particles (interaction sites) in space, which can be readily obtained from a PDB structure or a modeled protein. An important aspect of NMA is that all the modes are calculated as fluctuations in the proximity of a minimum-energy configuration. Therefore, the calculated modes are only correct near the initial equilibrium structure.[98] Furthermore, the method assumes that the fluctuations can be calculated using simple harmonic potentials.

2.6.1. Application Example I: Calculating Normal Modes in a Two-State Anisotropic Network Model. In a noteworthy study,[102] Das et al. introduced a simplified approach for modeling conformational transitions in biomolecules using the two-state anisotropic network model (2s-ANM). The method builds on the traditional anisotropic network model (ANM) but

https://doi.org/10.1021/acs.jpcb.5c00104
J. Phys. Chem. B 2025, 129, 3703−3719

focuses on capturing the essential collective motions between two distinct conformational states. By approximating the system as transitioning between two states, the 2s-ANM reduces computational complexity while still effectively capturing the anisotropic, directionally biased motions that drive the transition. In the study, 2s-ANM successfully captured transitions between the OF and IF states of the bacterial sodium-coupled leucine transporter (LeuT), as well as the formation of the OC states, which are highlights of the substrate transport cycle in transporters (Figure 7A-C). However, the two-state approach may not fully capture the nuanced, multistep nature of the transitions, as it ignores intermediate conformations and finer details. Furthermore, the model's focus on anisotropic motions may miss nonlinear or localized deformations, and like other network models, it assumes rigidity, neglecting the effects of solvent and other elements of the environment that may be important under cellular conditions.

2.6.2. Application Example II: Normal Mode-Guided Collective MD. In another study, authors employed a method, termed collective MD, to explore the energy landscape of LeuT.[103] collective MD is a hybrid method that simulates the dynamics of the system by biasing the structure along the modes predicted by ANM. This method combines the efficiency of ANM-guided collective dynamics with more localized dynamics described through MD simulations. The conformational changes are driven by a Monte Carlo/Metropolis algorithm, with steps repeated until a predefined deformation is achieved. This process generates an intermediate or "on-pathway" conformer, which is then further refined using targeted MD[104] (Figure 7E-F). The combination of multiple microseconds-long MD simulations with the collective MD approach yielded the free-energy landscape underlying the transition pathway involved in LeuT (Figure 7E,F).

It is important to note that the captured normal modes are described by the overall architecture of the protein (i.e., distribution of residues or backbone conformations). The slowest modes obtained from NMA can be used to capture global structural changes, while the local side-chain orientations fall usually outside this resolution limit. In order to access these local changes attention must be given to the region of interest and the modes that are specific to that region. This limitation can be alleviated partly by selecting an ensemble of frequency modes which can couple local and global conformational transitions.

2.6.3. Application Example III: Adaptive Bond Bending Elastic Network Model. A recent study developed and employed a bond-bending elasticity model in combination with ANM to study the conformational transition in LeuT.[105] This topology-based model that penalizes any bond-bending and bond-stretching motions highlighted the rearrangement of transmembrane helices and resulted in the closing of the extracellular side of LeuT followed by the opening of its intracellular side. The free-energy profiles calculated along the transition pathway captured the presence of multiple intermediates in the transitions cycle.

2.7. Brute-Force Molecular Dynamics. As discussed above, MD simulations incorporating user-defined biases or external forces and potentials have been widely utilized to drive and study the conformational changes between functional states of transporters. On the other hand, brute-force, unbiased MD simulations, performed on long time scales (multi-μs) have been also reported occasionally to capture transporters' transitions under equilibrium conditions.[106] Recent examples include multi-μs MD simulations utilized to shed light on a part of the transport cycle in heterodimeric ABC exporter TM287/288 from *Thermotoga maritima*, a bacterial homologue of drug efflux pump p-glycoprotein in humans. The study reports spontaneous conformational transitions between the IF and yet uncharacterized OC and OF states, as well as substrate translocation during the transition.[107,108] It should be noted that as this transporter belongs to a thermophile, MD simulations at 375 K could be justified allowing a faster transition between the different states over the time scale of the study.

In a similar study, utilizing multi-μs MD simulations, the conformational landscape of another transporter, glucose transporter 1 (GluT1), was explored both in the presence and absence of glucose, along with glucose translocation through the transporter during the process.[109] Notably, the conformational changes observed between the IF and OF states in that study involved relatively small orientational changes in the transmembrane helices, which is probably the reason why equilibrium simulations were able to describe them. Extended equilibrium simulations have also been successfully used to identify states and transitions in POTs.[110]

Recent advancements both in computer architecture and in software engineering are now making it possible to reach even longer simulation time scales more routinely, thereby increasing the chance of sampling functionally relevant conformational changes using just unbiased MD. Such MD simulations are, therefore, expected to be more frequently reported for describing relevant global motions in membrane transporters.

3. SOFTWARE TOOLS FOR MODELING LARGE-SCALE CONFORMATIONAL CHANGES

Modeling large-scale conformational changes in membrane transporters requires a robust MD simulation engine capable of simulating complex biomolecular processes through the application of CVs over extended time scales. Popular MD engines for such tasks include NAMD,[111,112] GROMACS,[113] CHARMM,[114] OpenMM,[115] AMBER,[116] and GENESIS.[117] These software packages provide the computational framework necessary to simulate membrane proteins, incorporating features such as lipid bilayers, solvent environments, and ion gradients. To overcome the time scale limitations of conventional MD, most of these engines support enhanced sampling methods through integration with the COLVARS (Collective Variables) module[36] and/or the PLUMED plugin.[118] These modules enable researchers to apply advanced techniques like metadynamics, ABF, driven MD, US, etc. which are essential for capturing rare events such as transporter conformational transitions. By leveraging these tools, one can gain mechanistic insights into the dynamics and function of membrane transporters at an atomic level.

4. CONCLUDING REMARKS AND FUTURE DIRECTIONS

Membrane transporters rely on large-scale structural changes to translocate their substrates from one side of the membrane to the other. Due to the complexity of these changes and the long time scales associated with them, their atomic-level characterization often requires the use of computational methods that are more advanced than standard equilibrium MD simulations. In this article, we provided an overview of a handful of advanced methods that have been successfully employed for describing the structural changes in membrane transporters.

https://doi.org/10.1021/acs.jpcb.5c00104
J. Phys. Chem. B 2025, 129, 3703−3719

The advanced methods described here all incorporate various forms of bias, often applied to distinct CVs, that induce the transporter's transition from one functional state to another. Care must be taken when defining these CVs to ensure that the pathways obtained from biased simulations closely resemble the ones used by nature. Conventionally, CVs have been defined based on a researcher's understanding of various biophysical and structural aspects of the transporter being studied.[8,29,119] However, machine learning methods have recently shown promise in helping define best CVs to use.[120−124] Artificial intelligence-based methods have been also used to predict distinct conformational states of membrane transporters and receptors.[125]

The reversibility of membrane transport generally suggests that the OF → IF conformational transition follows the same pathway as the IF → OF transition, except in reverse. However, it is theoretically possible that a particularly complex transporter mechanism could yield different OF → IF and IF → OF transition pathways. In such a scenario, the practice of CV discovery and enhanced sampling would need to be done independently for both directions.

When accelerating the movement of a membrane transporter, another important consideration is the lipid environment. All of the methods discussed here bias the dynamics of the protein, but the dynamics of the lipids are not usually directly biased, which can introduce inaccuracies into the simulation results if care is not taken.[126] Specific lipid−protein interactions can significantly affect the relative stability of a transporter's functional states,[127] which can influence the thermodynamics and kinetics of the entire transport cycle. For example, lipids have occasionally been observed to bind to the open mouths of transporters.[128−135] Such interactions can not only stabilize particular functional states of a transporter, but the binding/unbinding of these lipids constitutes an integral part of the transport cycle,[136] thus contributing to the cycle's overall time scale.

In nature, transporters are expected to operate in crowded cellular environments, conditions that are not reproduced in traditional simulations. A realistically crowded environment could certainly affect the overall dynamics of a membrane transporter as well as the energetics associated with its transport cycle. As the sophistication of modeling tools and power of computational resources improve, we expect that future simulations will represent the crowded environments membrane transporters experience within cells more realistically.

Finally, we expect that simulations will continue to benefit from the incorporation of experimental data from a variety of high-resolution techniques, including HDX-MS,[137] DEER,[129] NMR,[138] AFM, and FRET. These techniques provide atomistic information about the structures of individual functional states of transporters as well as the transitions between them, which may readily be used to guide the study of transporter function with simulations.

Detailed description of membrane transporters during their function is of direct ramifications not only in mechanistic biophysical studies, but also in drug discovery applications. Instead of having access to a single or a couple of experimental structures for docking studies of a membrane transporter,[139] simulations combined with AI-driven approaches would provide access to a plethora of protein structures[140,141] in the natural environment of a membrane to make predictions about putative binding and sites for small molecules and cryptic sites[142] that could be experimentally validated. Notably, one has to be mindful of the fact that the lifetime of some of the intermediates that arise during the transport cycle is short. In some cases, simulations have provided access to the structurally unknown states for docking studies.[143]

Despite the tremendous progress, we still have a long way to go until we comprehensively describe the natural motions of membrane transporters within their cellular environments. Structural and mechanistic studies of membrane transporters will continue to benefit from advances in experimental and computational techniques. Future studies will be able to provide more details on some of the fascinating aspects of the function of these molecular machines, for example, the structural coordination of the two ends of the protein that brings about the alternating access mechanism, or the chemomechanical coupling between chemical events such as ion/ligand binding/unbinding and the global structural changes.

AUTHOR INFORMATION

Corresponding Author

Emad Tajkhorshid − *Theoretical and Computational Biophysics Group, NIH Resource for Macromolecular Modeling and Visualization, Beckman Institute for Advanced Science and Technology, Department of Biochemistry, and Center for Biophysics and Quantitative Biology, University of Illinois Urbana−Champaign, Urbana, Illinois 61801-3028, United States;* orcid.org/0000-0001-8434-1010; Email: emad@illinois.edu

Authors

Shashank Pant − *Theoretical and Computational Biophysics Group, NIH Resource for Macromolecular Modeling and Visualization, Beckman Institute for Advanced Science and Technology, Department of Biochemistry, and Center for Biophysics and Quantitative Biology, University of Illinois Urbana−Champaign, Urbana, Illinois 61801-3028, United States;* Present Address: Current address: Eli Lilly, 600 Tech Ct, Louisville, Colorado 80027, U.S.A; orcid.org/0000-0002-8222-3616

Sepehr Dehghani-Ghahnaviyeh − *Theoretical and Computational Biophysics Group, NIH Resource for Macromolecular Modeling and Visualization, Beckman Institute for Advanced Science and Technology, Department of Biochemistry, and Center for Biophysics and Quantitative Biology, University of Illinois Urbana−Champaign, Urbana, Illinois 61801-3028, United States;* orcid.org/0000-0001-6113-3438

Noah Trebesch − *Theoretical and Computational Biophysics Group, NIH Resource for Macromolecular Modeling and Visualization, Beckman Institute for Advanced Science and Technology, Department of Biochemistry, and Center for Biophysics and Quantitative Biology, University of Illinois Urbana−Champaign, Urbana, Illinois 61801-3028, United States;* orcid.org/0000-0001-5536-4862

Ali Rasouli − *Theoretical and Computational Biophysics Group, NIH Resource for Macromolecular Modeling and Visualization, Beckman Institute for Advanced Science and Technology, Department of Biochemistry, and Center for Biophysics and Quantitative Biology, University of Illinois Urbana−Champaign, Urbana, Illinois 61801-3028, United States*

Tianle Chen − *Theoretical and Computational Biophysics Group, NIH Resource for Macromolecular Modeling and Visualization, Beckman Institute for Advanced Science and Technology, Department of Biochemistry, and Center for*

https://doi.org/10.1021/acs.jpcb.5c00104
J. Phys. Chem. B 2025, 129, 3703−3719

Biophysics and Quantitative Biology, University of Illinois Urbana−Champaign, Urbana, Illinois 61801-3028, United States; orcid.org/0000-0001-6581-8012

Karan Kapoor − *Theoretical and Computational Biophysics Group, NIH Resource for Macromolecular Modeling and Visualization, Beckman Institute for Advanced Science and Technology, Department of Biochemistry, and Center for Biophysics and Quantitative Biology, University of Illinois Urbana−Champaign, Urbana, Illinois 61801-3028, United States*

Po-Chao Wen − *Theoretical and Computational Biophysics Group, NIH Resource for Macromolecular Modeling and Visualization, Beckman Institute for Advanced Science and Technology, Department of Biochemistry, and Center for Biophysics and Quantitative Biology, University of Illinois Urbana−Champaign, Urbana, Illinois 61801-3028, United States;* orcid.org/0000-0002-6049-6904

Complete contact information is available at: https://pubs.acs.org/10.1021/acs.jpcb.5c00104

Author Contributions

†(S.P., S.D.-G.) Contributed equally to this work.

Notes

The authors declare no competing financial interest.

Biographies

Shashank Pant earned his PhD in 2021 from University of Illinois Urbana−Champaign (UIUC). His research focuses on leveraging classical mechanical simulation methods to investigate the kinetics and thermodynamics of complex biological processes. Specifically, Shashank develops and applies advanced all-atom simulations to study biomolecular dynamics at millisecond time scales and beyond, bridging the gap between theoretical models and experimental observations. To overcome the limitations of traditional computational approaches, he employs enhanced sampling algorithms to explore the conformational dynamics of biomedically relevant molecules. His work aims to uncover fundamental insights into biomolecular behavior, enabling the rational design of novel therapeutics and small molecules with potential applications in drug discovery and biomedical engineering.

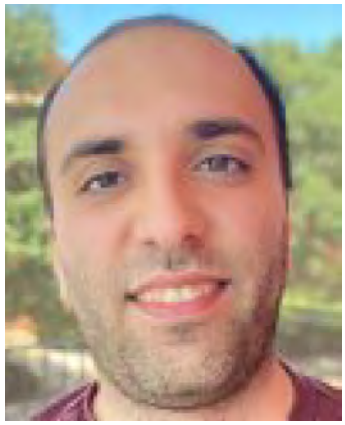

Dr Dehghani-Ghahnaviyeh is a Senior Scientist at Novartis Biomedical Research. He received his PhD in 2022 from UIUC. His research focuses on using in-silico techniques to understand biological systems and design novel therapeutics.

Noah Trebesch is currently a postdoctoral researcher in the lab of Emad Tajkhorshid at UIUC, where he also completed his PhD in Biophysics and Computational Biology in 2023. He previously received a BS in Physics (Biological Physics emphasis) and a BS in Computer Science (Computational Science emphasis) from the University of Minnesota - Twin Cities. In his research, Noah uses advanced molecular dynamics simulation techniques to structurally and thermodynamically characterize the mechanisms of transporters, and he uses comparative structural analyses to investigate the phylogenetics and evolution of transporters. He also develops new approaches to atomistically model and simulate cell-scale membrane systems with realistically complex curvature and lipid compositions.

Ali Rasouli is currently a postdoctoral researcher at BIOVIA, and he received his Ph.D. from UIUC, where he applied advanced molecular simulations to study biomolecular systems. His current research focuses

on integrating physics-based techniques with data-driven methods, including AI and machine learning, to enhance the modeling and understanding of complex biological systems.

Tianle Chen is a PhD student in Biophysics at UIUC, working in the lab of Emad Tajkhorshid. His research focuses on membrane proteins, including transporters and channels, with an emphasis on using enhanced sampling techniques to investigate their conformational dynamics.

Karan Kapoor is a Senior Computational Chemist at Ensem Therapeutics. He earned his Ph.D. in Molecular Biophysics from the University of Tennessee and Oak Ridge National Laboratory, followed by postdoctoral research at the University of Illinois Urbana−Champaign. His research combines molecular dynamics simulations, enhanced sampling techniques, and structure-based drug design to investigate biomolecular mechanisms and advance therapeutic discovery.

Po-Chao Wen is a Research Scientist of the NIH Resource for Macromolecular Modeling and Visualization at the University of Illinois Urbana−Champaign. His research includes molecular dynamics studies of the mechanism of various membrane transporters and the mode of action on several antimicrobial compounds.

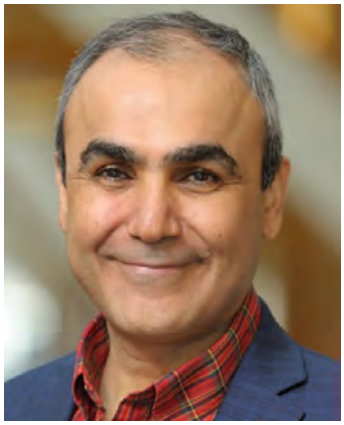

Emad Tajkhorshid is Hastings Endowed Chair in the Biochemistry Department and holds additional appointments across multiple colleges that include Chemistry, Bioengineering, Pharmacology, Biophysics and Quantitative Biology, Computational Science and Engineering, and the Carle-Illinois College of Medicine at UIUC. He received his Pharm.D. from Tehran University and a Ph.D. in molecular biophysics from the University of Heidelberg, before moving to the UIUC, where he did his postdoctoral studies at the Beckman Institute. He joined the faculty of the Biochemistry (LAS) and Pharmacology (UI COM) in 2007 and was fast tracked to associate professor with tenure in 2010 and then again to the rank of professor in 2013. His tenure dossier was selected as one of the two top UIUC tenure cases on campus. In 2015, he was named a University of Illinois Scholar, after being nominated by both UIUC and UIC campuses. In 2016, he was awarded the Faculty Excellence Award from the School of Molecular and Cellular Biology at UIUC. Later that year he was named Endowed Chair in Biochemistry. He was awarded the Research Excellence Award from the School of Molecular and Cellular Biology at UIUC in 2022. He is a world leader in developing and applying advanced computational techniques to characterization of membrane proteins, with the aim of achieving the most detailed microscopic view of structural and dynamical bases underlying their biological function. Major areas of his extensive research portfolio, which have enjoyed continuous support from multiple federal funding agencies (NIH, NSF, DOE, DOD) over decades, include mechanistic studies of membrane transport proteins and lipid modulation of protein function. He has authored over 330 research articles with nearly 47,000 citations (Google H-index 87).

■ ACKNOWLEDGMENTS

The authors acknowledge support from the National Institutes of Health (NIH) through grants P41-GM104601, R24-GM145965, R01-DK128315, R01-GM145783, R01-NS126584, and R01-DK135088, as well as the National Science Foundation (NSF) Science and Technology Center for Quantitative Cell Biology (grant 2218365). We also acknowledge the computational resources provided by the NSF Supercomputing Centers (ACCESS grant number MCA06N060) and Delta advanced computing and data resource which is supported by NSF (award OAC 2005572) and the State of Illinois.

https://doi.org/10.1021/acs.jpcb.5c00104
J. Phys. Chem. B 2025, 129, 3703−3719

REFERENCES

(1) Dror, R. O.; Dirks, R. M.; Grossman, J.; Xu, H.; Shaw, D. E. Biomolecular Simulation: A Computational Microscope for Molecular Biology. *Annu. Rev. Biophys.* **2012**, *41*, 429−452.

(2) Bernardi, R. C.; Melo, M. C. R.; Schulten, K. Enhanced Sampling Techniques in Molecular Dynamics Simulations of Biological Systems. *Biochim. Biophys. Acta* **2015**, *1850*, 872−877.

(3) Saladino, G.; Gervasio, F. L. Modeling the effect of pathogenic mutations on the conformational landscape of protein kinases. *Curr. Opin. Struct. Biol.* **2016**, *37*, 108−114.

(4) Flood, E.; Boiteux, C.; Lev, B.; Vorobyov, I.; Allen, T. W. Atomistic Simulations of Membrane Ion Channel Conduction, Gating, and Modulation. *Chem. Rev.* **2019**, *119*, 7737−7832.

(5) Acharya, A.; Prajapati, J. D.; Kleinekathöfer, U. Improved Sampling and Free Energy Estimates for Antibiotic Permeation Through Bacterial Porins. *J. Chem. Theory Comput.* **2021**, *17*, 4564−4577.

(6) Vasan, A. K.; Haloi, N.; Ulrich, R. J.; Metcalf, M. E.; Wen, P.-C.; Metcalf, W. W.; Hergenrother, P. J.; Shukla, D.; Tajkhorshid, E. Role of Internal Loop Dynamics in Antibiotic Permeability of Outer Membrane Porins. *Proc. Natl. Acad. Sci. U.S.A.* **2022**, *119*, No. e2117009119.

(7) Chen, I.; Pant, S.; Wu, Q.; Cater, R.; Sobti, M.; Vandenberg, R.; Stewart, A. G.; Tajkhorshid, E.; Font, J.; Ryan, R. Glutamate Transporters Have a Chloride Channel with Two Hydrophobic Gates. *Nature* **2021**, *591*, 327−331.

(8) Moradi, M.; Enkavi, G.; Tajkhorshid, E. Atomic-level Characterization of Transport Cycle Thermodynamics in the Glycerol-3-phosphate:phosphate Transporter. *Nat. Commun.* **2015**, *6*, 8393.

(9) Lichtinger, S. M.; Biggin, P. C. Tackling Hysteresis in Conformational Sampling: How to Be Forgetful with Memento. *J. Chem. Theory Comput.* **2023**, *19*, 3705−3720.

(10) Meshkin, H.; Zhu, F. Toward Convergence in Free Energy Calculations for Protein Conformational Changes: A case Study on the Thin Gate of Mhp1 transporter. *J. Chem. Theory Comput.* **2021**, *17*, 6583−6596.

(11) Pant, S.; Wu, Q.; Ryan, R.; Tajkhorshid, E. Microscopic Characterization of the Chloride Permeation Pathway in the Human Excitatory Amino Acid Transporter 1 (EAAT1). *ACS Chem. Neurosci.* **2022**, *13*, 776−785.

(12) Bruce, N. J.; Ganotra, G. K.; Kokh, D. B.; Sadiq, S. K.; Wade, R. C. New approaches for computing ligand-receptor binding kinetics. *Curr. Opin. Struct. Biol.* **2018**, *49*, 1−10.

(13) Liu, Z.; Cao, X.; Ma, Z.; Xu, L.; Wang, L.; Li, J.; Xiao, M.; Jiang, X. Enhanced Sampling Molecular Dynamics Simulations Reveal Transport Mechanism of Glycoconjugate Drugs through GLUT1. *Int. J. Mol. Sci.* **2024**, *25*, 5486.

(14) Janoš, P.; Magistrato, A. Role of Monovalent Ions in the NKCC1 Inhibition Mechanism Revealed through Molecular Simulations. *Int. J. Mol. Sci.* **2022**, *23*, 15439.

(15) Ikebe, J.; Umezawa, K.; Higo, J. Enhanced sampling simulations to construct free-energy landscape of protein-partner substrate interaction. *Biophys. Rev.* **2016**, *8*, 45−62.

(16) Drew, D.; Boudker, O. Shared Molecular Mechanisms of Membrane Transporters. *Annu. Rev. Biochem.* **2016**, *85*, 543−572.

(17) Mitchell, P. A. General Theory of Membrane Transport From Studies of Bacteria. *Nature* **1957**, *180*, 134−136.

(18) Jardetzky, O. Simple Allosteric Model for Membrane Pumps. *Nature* **1966**, *211*, 969−970.

(19) Bosshart, P. D.; Fotiadis, D. Secondary Active Transporters. In *Bacterial Cell Walls and Membranes*; Kuhn, A., Ed.; Subcellular Biochemistry Book Series; Springer: Cham, Switzerland, 2019; Vol. 92; pp 275−299.

(20) Alam, A.; Locher, K. P. Structure and Mechanism of Human ABC Transporters. *Annu. Rev. Biophys.* **2023**, *52*, 275−300.

(21) Lisal, J.; Maduke, M. The ClC-0 Chloride Channel Is a 'broken' Cl^-/H^+ Antiporter. *Nat. Struct. Mol. Biol.* **2008**, *15*, 805−810.

(22) Suades, A.; Qureshi, A.; McComas, S. E.; Coinçon, M.; Rudling, A.; Chatzikyriakidou, Y.; Landreh, M.; Carlsson, J.; Drew, D. Establishing Mammalian GLUT Kinetics and Lipid Composition Influences in a Reconstituted-liposome System. *Nat. Commun.* **2023**, *14*, 4070.

(23) Ruan, Y.; Miyagi, A.; Wang, X.; Chami, M.; Boudker, O.; Scheuring, S. Direct Visualization of Glutamate Transporter Elevator Mechanism by High-speed AFM. *Proc. Natl. Acad. Sci. U.S.A.* **2017**, *114*, 1584−1588.

(24) Okazaki, K.-i.; Wöhlert, D.; Warnau, J.; Jung, H.; Yildiz, Ö.; Kühlbrandt, W.; Hummer, G. Mechanism of the electroneutral sodium/proton antiporter PaNhaP from transition-path shooting. *Nat. Commun.* **2019**, *10*, 1742.

(25) Rogal, J.; Bolhuis, P. G. Multiple state transition path sampling. *J. Chem. Phys.* **2008**, *129*, 129.

(26) Jung, H.; Okazaki, K.-i.; Hummer, G. Transition path sampling of rare events by shooting from the top. *J. Chem. Phys.* **2017**, *147*, 152716 DOI: 10.1063/1.4997378.

(27) Faradjian, A. K.; Elber, R. Computing time scales from reaction coordinates by milestoning. *J. Chem. Phys.* **2004**, *120*, 10880−10889.

(28) Zuckerman, D. M.; Chong, L. T. Weighted ensemble simulation: review of methodology, applications, and software. *Annual review of biophysics* **2017**, *46*, 43−57.

(29) Moradi, M.; Tajkhorshid, E. Mechanistic Picture for Conformational Transition of a Membrane Transporter at Atomic Resolution. *Proc. Natl. Acad. Sci. U.S.A.* **2013**, *110*, 18916−18921.

(30) Moradi, M.; Tajkhorshid, E. Computational Recipe for Efficient Description of Large-scale Conformational Changes in Biomolecular Systems. *J. Chem. Theory Comput.* **2014**, *10*, 2866−2880.

(31) Sauer, D. B.; Trebesch, N.; Marden, J. J.; Cocco, N.; Song, J.; Koide, A.; Koide, S.; Tajkhorshid, E.; Wang, D.-N. Structural Basis for the Reaction Cycle of DASS Dicarboxylate Transporters. *eLife* **2020**, *9*, No. e61350.

(32) Tamura, K.; Sugita, Y. Free Energy Analysis of a Conformational Change of Heme ABC Transporter BhuUV-T. *J. Phys. Chem. Lett.* **2020**, *11*, 2824−2829.

(33) Trabuco, L. G.; Villa, E.; Mitra, K.; Frank, J.; Schulten, K. Flexible Fitting of Atomic Structures into Electron Microscopy Maps Using Molecular Dynamics. *Structure* **2008**, *16*, 673−683.

(34) Fiser, A.; Šali, A. Modeller: Generation and Refinement of Homology-based Protein Structure Models. *Meth. Enzym.* **2003**, *374*, 461−491.

(35) Vergara-Jaque, A.; Fenollar-Ferrer, C.; Kaufmann, D.; Forrest, L. R. Repeat-swap homology modeling of secondary active transporters: updated protocol and prediction of elevator-type mechanisms. *Frontiers in Pharmacology* **2015**, *6*, 183.

(36) Fiorin, G.; Klein, M. L.; Hénin, J. Using Collective Variables to Drive Molecular Dynamics Simulations. *Mol. Phys.* **2013**, *111*, 3345−3362.

(37) Izrailev, S.; Stepaniants, S.; Balsera, M.; Oono, Y.; Schulten, K. Molecular Dynamics Study of Unbinding of the Avidin-Biotin Complex. *Biophys. J.* **1997**, *72*, 1568−1581.

(38) Vermaas, J. V.; Rempe, S. B.; Tajkhorshid, E. Electrostatic Lock in the Transport Cycle of the Multi-Drug Resistance Transporter EmrE. *Proc. Natl. Acad. Sci. U.S.A.* **2018**, *115*, E7502−E7511.

(39) Li, J.; Zhao, Z.; Tajkhorshid, E. Locking Two Rigid-body Bundles in an Outward-Facing Conformation: A General Ion-coupling Mechanism in LeuT-fold Transporters. *Sci. Rep.* **2019**, *9*, 19479.

(40) Pan, A. C.; Sezer, D.; Roux, B. Finding Transition Pathways Using the String Method with Swarms of Trajectories. *J. Phys. Chem. B* **2008**, *112*, 3432−3440.

(41) Rui, H.; Das, A.; Nakamoto, R.; Roux, B. Proton Countertransport and Coupled Gating in the Sarcoplasmic Reticulum Calcium Pump. *J. Mol. Biol.* **2018**, *430*, 5050−5065.

(42) McComas, S. E.; Reichenbach, T.; Mitrovic, D.; Alleva, C.; Bonaccorsi, M.; Delemotte, L.; Drew, D. Determinants of Sugar-induced Influx in the Mammalian Fructose Transporter GLUT5. *eLife* **2023**, *12*, No. e84808.

(43) Torrie, G. M.; Valleau, J. P. Nonphysical Sampling Distributions in Monte Carlo Free-energy Estimation: Umbrella Sampling. *J. Comput. Phys.* **1977**, *23*, 187−199.

(44) Northrup, S. H.; Pear, M. R.; Lee, C. Y.; McCammon, J. A.; Karplus, M. Dynamical Theory of Activated Processes in Globular Proteins. *Proc. Natl. Acad. Sci. U.S.A.* **1982**, *79*, 4035−4039.
(45) Kumar, S.; Bouzida, D.; Swendsen, R. H.; Kollman, P. A.; Rosenberg, J. M. THE Weighted Histogram Analysis Method for Free-energy Calculations on Biomolecules. I. The Method. *J. Comput. Chem.* **1992**, *13*, 1011−1021.
(46) Shirts, M. R.; Chodera, J. D. Statistically Optimal Analysis of Samples From Multiple Equilibrium States. *J. Chem. Phys.* **2008**, *129*, 124105.
(47) Sugita, Y.; Kitao, A.; Okamoto, Y. Multidimensional Replica-exchange Method for Free-energy Calculations. *J. Chem. Phys.* **2000**, *113*, 6042−6051.
(48) Matsunaga, Y.; Yamane, T.; Terada, T.; Moritsugu, K.; Fujisaki, H.; Murakami, S.; Ikeguchi, M.; Kidera, A. Energetics and Conformational Pathways of Functional Rotation in the Multidrug Transporter AcrB. *eLife* **2018**, *7*, No. e31715.
(49) Laio, A.; Parrinello, M. Escaping Free Energy Minima. *Proc. Natl. Acad. Sci. U.S.A.* **2002**, *99*, 12562−12566.
(50) Laio, A.; Rodriguez-Fortea, A.; Gervasio, F. L.; Ceccarelli, M.; Parrinello, M. Assessing the Accuracy of Metadynamics. *J. Phys. Chem. B* **2005**, *109*, 6714−6721.
(51) Barducci, A.; Bussi, G.; Parrinello, M. Well-Tempered Metadynamics: A Smoothly Converging and Tunable Free-Energy Method. *Phys. Rev. Lett.* **2008**, *100*, 020603.
(52) Masrati, G.; Mondal, R.; Rimon, A.; Kessel, A.; Padan, E.; Lindahl, E.; Ben-Tal, N. An Angular Motion of a Conserved Four-helix Bundle Facilitates Alternating Access Transport in the TtNapA and EcNhaA Transporters. *Proc. Natl. Acad. Sci. U.S.A.* **2020**, *117*, 31850−31860.
(53) Bussi, G.; Gervasio, F. L.; Laio, A.; Parrinello, M. Free-energy landscape for β hairpin folding from combined parallel tempering and metadynamics. *J. Am. Chem. Soc.* **2006**, *128*, 13435−13441.
(54) Tiwary, P.; Parrinello, M. From metadynamics to dynamics. *Phys. Rev. Lett.* **2013**, *111*, 230602.
(55) Chakrabarti, M.; Amzel, L. M.; Lau, A. Y. Sodium/Iodide Symporter Metastable Intermediates Provide Insights into Conformational Transition between Principal Thermodynamic States. *J. Phys. Chem. B* **2023**, *127*, 1540−1551.
(56) Lu, X.; Huang, J. Molecular Mechanisms of Na+-driven Bile Acid Transport in Human NTCP. *Biophys. J.* **2024**, *123*, 1195−1210.
(57) Janoš, P.; Aupič, J.; Ruthstein, S.; Magistrato, A. The Conformational Plasticity of the Selectivity Filter Methionines Controls the In-cell Cu(I) Uptake Through the CTR1 Transporter. *QRB Discovery* **2022**, *3*, No. e3.
(58) Janos, P.; Magistrato, A. All-atom Simulations Uncover the Molecular Terms of the NKCC1 Transport Mechanism. *J. Chem. Inf. Model.* **2021**, *61*, 3649−3658.
(59) Comer, J.; Gumbart, J. C.; Hénin, J.; Lelièvre, T.; Pohorille, A.; Chipot, C. The Adaptive Biasing Force Method: Everything You Always Wanted to Know but Were Afraid to Ask. *J. Phys. Chem. B* **2015**, *119*, 1129−1151.
(60) Lesage, A.; Lelievre, T.; Stoltz, G.; Hénin, J. Smoothed Biasing Forces Yield Unbiased Free Energies with the Extended-system Adaptive Biasing Force Method. *J. Phys. Chem. B* **2017**, *121*, 3676−3685.
(61) Fu, H.; Shao, X.; Cai, W.; Chipot, C. Taming Rugged Free Energy Landscapes Using an Average Force. *Acc. Chem. Res.* **2019**, *52*, 3254−3264.
(62) Fu, H.; Shao, X.; Chipot, C.; Cai, W. Extended Adaptive Biasing Force Algorithm. An On-the-fly Implementation for Accurate Free-energy Calculations. *J. Chem. Theory Comput.* **2016**, *12*, 3506−3513.
(63) Zhao, T.; Fu, H.; Lelièvre, T.; Shao, X.; Chipot, C.; Cai, W. The Extended Generalized Adaptive Biasing Force Algorithm for Multi-dimensional Free-energy Calculations. *J. Chem. Theory Comput.* **2017**, *13*, 1566−1576.
(64) Batista, M. R.; Watts, A.; José Costa-Filho, A. Exploring Conformational Transitions and Free-energy Profiles of Proton-coupled Oligopeptide Transporters. *J. Chem. Theory Comput.* **2019**, *15*, 6433−6443.
(65) Darve, E.; Rodríguez-Gómez, D.; Pohorille, A. Adaptive Biasing Force Method for Scalar and Vector Free Energy Calculations. *J. Chem. Phys.* **2008**, *128*, 144120.
(66) Lee, C. T.; Comer, J.; Herndon, C.; Leung, N.; Pavlova, A.; Swift, R. V.; Tung, C.; Rowley, C. N.; Amaro, R. E.; Chipot, C.; et al. Simulation-based Approaches for Determining Membrane Permeability of Small Compounds. *J. Chem. Inf. Model.* **2016**, *56*, 721−733.
(67) Comer, J.; Schulten, K.; Chipot, C. Calculation of Lipid-Bilayer Permeabilities Using an Average Force. *J. Chem. Theory Comput.* **2014**, *10*, 554−564.
(68) Comer, J.; Dehez, F.; Cai, W.; Chipot, C. Water Conduction Through a Peptide Nanotube. *J. Phys. Chem. C* **2013**, *117*, 26797−26803.
(69) Hazel, A.; Chipot, C.; Gumbart, J. C. Thermodynamics of Deca-alanine Folding in Water. *J. Chem. Theory Comput.* **2014**, *10*, 2836−2844.
(70) Cheng, M. H.; Kaya, C.; Bahar, I. Quantitative Assessment of the Energetics of Dopamine Translocation by Human Dopamine Transporter. *J. Phys. Chem. B* **2018**, *122*, 5336−5346.
(71) Miao, Y.; Sinko, W.; Pierce, L.; Bucher, D.; Walker, R. C.; McCammon, J. A. Improved Reweighting of Accelerated Molecular Dynamics Simulations for Free Energy Calculation. *J. Chem. Theory Comput.* **2014**, *10*, 2677−2689.
(72) Kappel, K.; Miao, Y.; McCammon, J. A. Accelerated Molecular Dynamics Simulations of Ligand Binding to a Muscarinic G-protein Coupled Receptor. *Q. Rev. Biophys.* **2015**, *48*, 479−487.
(73) Miao, Y.; Feher, V. A.; McCammon, J. A. Gaussian Accelerated Molecular Dynamics: Unconstrained Enhanced Sampling and Free Energy Calculation. *J. Chem. Theory Comput.* **2015**, *11*, 3584−3595.
(74) Bhattarai, A.; Wang, J.; Miao, Y. G-protein-coupled Receptor−membrane Interactions Depend on the Receptor Activation State. *J. Comput. Chem.* **2020**, *41*, 460−471.
(75) Wang, J.; Miao, Y. Peptide Gaussian Accelerated Molecular Dynamics (Pep-GaMD): Enhanced Sampling and Free Energy and Kinetics Calculations of Peptide Binding. *J. Chem. Phys.* **2020**, *153*, 154109.
(76) Miao, Y.; Bhattarai, A.; Wang, J. Ligand Gaussian Accelerated Molecular Dynamics (LiGaMD): Characterization of Ligand Binding Thermodynamics and Kinetics. *J. Chem. Theory Comput.* **2020**, *16*, 5526−5547.
(77) Wang, W.; Cao, S.; Zhu, L.; Huang, X. Constructing Markov State Models to Elucidate the Functional Conformational Changes of Complex Biomolecules. *Wiley Interdiscip. Rev.: Comput. Mol. Sci.* **2018**, *8*, No. e1343.
(78) Lane, T. J.; Shukla, D.; Beauchamp, K. A.; Pande, V. S. To Milliseconds and Beyond: Challenges in the Simulation of Protein Folding. *Curr. Opin. Struct. Biol.* **2013**, *23*, 58−65.
(79) Husic, B. E.; Pande, V. S. Markov State Models: From an Art to a Science. *J. Am. Chem. Soc.* **2018**, *140*, 2386−2396.
(80) Shukla, D.; Hernández, C. X.; Weber, J. K.; Pande, V. S. Markov State Models Provide Insights into Dynamic Modulation of Protein Function. *Acc. Chem. Res.* **2015**, *48*, 414−422.
(81) Bowman, G. R.; Ensign, D. L.; Pande, V. S. Enhanced Modeling via Network Theory: Adaptive Sampling of Markov State Models. *J. Chem. Theory Comput.* **2010**, *6*, 787−794.
(82) Selvam, B.; Mittal, S.; Shukla, D. Free Energy Landscape of the Complete Transport Cycle in a Key Bacterial Transporter. *ACS Cent. Sci.* **2018**, *4*, 1146−1154.
(83) Harrigan, M. P.; Sultan, M. M.; Hernández, C. X.; Husic, B. E.; Eastman, P.; Schwantes, C. R.; Beauchamp, K. A.; McGibbon, R. T.; Pande, V. S. MSMBuilder: Statistical Models for Biomolecular Dynamics. *Biophys. J.* **2017**, *112*, 10−15.
(84) Scherer, M. K.; Trendelkamp-Schroer, B.; Paul, F.; Pérez-Hernández, G.; Hoffmann, M.; Plattner, N.; Wehmeyer, C.; Prinz, J.-H.; Noé, F. PyEMMA 2: A Software Package for Estimation, Validation, and Analysis of Markov Models. *J. Chem. Theory Comput.* **2015**, *11*, 5525−5542.

https://doi.org/10.1021/acs.jpcb.5c00104
J. Phys. Chem. B 2025, 129, 3703−3719

(85) Latorraca, N. R.; Masureel, M.; Hollingsworth, S. A.; Heydenreich, F. M.; Suomivuori, C.-M.; Brinton, C.; Townshend, R. J.; Bouvier, M.; Kobilka, B. K.; Dror, R. O. How GPCR Phosphorylation Patterns Orchestrate Arrestin-Mediated Signaling. *Cell* **2020**, *183*, 1813−1825.
(86) Barros, E. P.; Demir, Ö.; Soto, J.; Cocco, M. J.; Amaro, R. E. Markov state models and NMR uncover an overlooked allosteric loop in p53. *Chem. Sci.* **2021**, *12*, 1891−1900.
(87) Paul, F.; Meng, Y.; Roux, B. Identification of Druggable Kinase Target Conformations Using Markov Model Metastable States Analysis of apo-Abl. *J. Chem. Theory Comput.* **2020**, *16*, 1896−1912.
(88) Thomas, T.; Yuriev, E.; Chalmers, D. K. Markov State Model Analysis of Haloperidol Binding to the D3 Dopamine Receptor. *J. Chem. Theory Comput.* **2020**, *16*, 3879−3888.
(89) Weigle, A. T.; Shukla, D. The Arabidopsis AtSWEET13 Transporter Discriminates Sugars by Selective Facial and Positional Substrate Recognition. *Commun. Biol.* **2024**, *7*, 764.
(90) Alves da Silva, L.; Lazzarin, E.; Gradisch, R.; Clarke, A.; Stockner, T. Free Energy Profile of the Substrate-induced Occlusion of the Human Serotonin Transporter. *J. Neurochem.* **2024**, *168*, 1993−2006.
(91) Chan, M. C.; Shukla, D. Markov State Modeling of Membrane Transport Proteins. *J. Struct. Biol.* **2021**, *213*, 107800.
(92) Feng, J.; Selvam, B.; Shukla, D. How Do Antiporters Exchange Substrates Across the Cell Membrane? An Atomic-level Description of the Complete Exchange Cycle in NarK. *Structure* **2021**, *29*, 922−933.
(93) Quiroz, R.; Philot, E.; General, I.; Perahia, D.; Scott, A. Effect of Phosphorylation on the Structural Dynamics, Thermal Stability of Human Dopamine Transporter: A Simulation Study Using Normal Modes, Molecular Dynamics and Markov State Model. *J. Mol. Graph. Model.* **2023**, *118*, 108359.
(94) Cheng, K. J.; Selvam, B.; Chen, L.-Q.; Shukla, D. Distinct Substrate Transport Mechanism Identified in Homologous Sugar Transporters. *J. Phys. Chem. B* **2019**, *123*, 8411−8418.
(95) Klepeis, J. L.; Lindorff-Larsen, K.; Dror, R. O.; Shaw, D. E. Long-timescale Molecular Dynamics Simulations of Protein Structure and Function. *Curr. Opin. Struct. Biol.* **2009**, *19*, 120−127.
(96) Wingert, B.; Krieger, J.; Li, H.; Bahar, I. Adaptability and specificity: how do proteins balance opposing needs to achieve function? *Curr. Opin. Struct. Biol.* **2021**, *67*, 25−32.
(97) Bahar, I.; Lezon, T. R.; Yang, L. W.; Eyal, E. Global Dynamics of Proteins: Bridging Between Structure and Function. *Annu. Rev. Biophys.* **2010**, *39*, 23−42.
(98) Bahar, I.; Lezon, T. R.; Bakan, A.; Shrivastava, I. H. Normal Mode Analysis of Biomolecular Structures: Functional Mechanisms of Membrane Proteins. *Chem. Rev.* **2010**, *110*, 1463−1497.
(99) Ma, J. Usefulness and Limitations of Normal Mode Analysis in Modeling Dynamics of Biomolecular Complexes. *Structure* **2005**, *13*, 373−380.
(100) Souza, P. C.; Alessandri, R.; Barnoud, J.; Thallmair, S.; Faustino, I.; Grünewald, F.; Patmanidis, I.; Abdizadeh, H.; Bruininks, B. M.; Wassenaar, T. A.; et al. Martini 3: a General Purpose Force Field for Coarse-grained Molecular Dynamics. *Nat. Methods* **2021**, *18*, 382−388.
(101) Lopez-Rodriguez, E.; Pérez-Gil, J. Structure-function Relationships in Pulmonary Surfactant Membranes: From Biophysics to Therapy. *Biochim. Biophys. Acta* **2014**, *1838*, 1568−85.
(102) Das, A.; Gur, M.; Cheng, M. H.; Jo, S.; Bahar, I.; Roux, B. Exploring the Conformational Transitions of Biomolecular Systems Using a Simple Two-state Anisotropic Network Model. *PLoS Comput. Biol.* **2014**, *10*, No. e1003521.
(103) Gur, M.; Zomot, E.; Cheng, M. H.; Bahar, I. Energy Landscape of LeuT From Molecular Simulations. *J. Chem. Phys.* **2015**, *143*, 12B6111.
(104) Gur, M.; Madura, J. D.; Bahar, I. Global transitions of proteins explored by a multiscale hybrid methodology: application to adenylate kinase. *Biophys. J.* **2013**, *105*, 1643−1652.
(105) Srivastava, A. Conformational Transitions of Bio-molecular Systems Studied Using Adaptive Bond Bending Elastic Network Model. *J. Chem. Phys.* **2019**, *151*, 065101.
(106) Immadisetty, K.; Hettige, J.; Moradi, M. Lipid-dependent Alternating Access Mechanism of a Bacterial Multidrug ABC Exporter. *ACS Cent. Sci.* **2019**, *5*, 43−56.
(107) Göddeke, H.; Timachi, M. H.; Hutter, C. A. J.; Galazzo, L.; Seeger, M. A.; Karttunen, M.; Bordignon, E.; Schäfer, L. V. Atomistic Mechanism of Large-Scale Conformational Transition in a Heterodimeric ABC Exporter. *J. Am. Chem. Soc.* **2018**, *140*, 4543−4551.
(108) Göddeke, H.; Schäfer, L. V. Capturing Substrate Translocation in an ABC Exporter at the Atomic Level. *J. Am. Chem. Soc.* **2020**, *142*, 12791−12801.
(109) Galochkina, T.; Chong, M. N. F.; Challali, L.; Abbar, S.; Etchebest, C. New Insights into GluT1Mechanics During Glucose Transfer. *Sci. Rep.* **2019**, *9*, 1−14.
(110) Lichtinger, S. M.; Parker, J. L.; Newstead, S.; Biggin, P. C. The Mechanism of Mammalian Proton-coupled Peptide Transporters. *eLife* **2024**, *13*, RP96507.
(111) Phillips, J. C.; Braun, R.; Wang, W.; Gumbart, J.; Tajkhorshid, E.; Villa, E.; Chipot, C.; Skeel, R. D.; Kale, L.; Schulten, K. Scalable Molecular Dynamics with NAMD. *J. Comput. Chem.* **2005**, *26*, 1781−1802.
(112) Phillips, J. C.; Hardy, D. J.; Maia, J. D. C.; Stone, J. E.; Ribeiro, J. V.; Bernardi, R. C.; Buch, R.; Fiorin, G.; Hénin, J.; Jiang, W.; et al. Scalable Molecular Dynamics on CPU and GPU Architectures with NAMD. *J. Chem. Phys.* **2020**, *153*, 044130.
(113) Abraham, M. J.; Murtola, T.; Schulz, R.; Páll, S.; Smith, J. C.; Hess, B.; Lindahl, E. GROMACS: High Performance Molecular Simulations Through Multi-level Parallelism From Laptops to Supercomputers. *SoftwareX* **2015**, *1*, 19−25.
(114) Brooks, B. R.; Brooks, C. L.; Mackerell, A. D.; Nilsson, L.; Petrella, R. J.; Roux, B.; Won, Y.; Archontis, G.; Bartels, C.; Boresch, S.; et al. CHARMM: The Biomolecular Simulation Program. *J. Comput. Chem.* **2009**, *30*, 1545−1614.
(115) Eastman, P.; Swails, J.; Chodera, J. D.; McGibbon, R. T.; Zhao, Y.; Beauchamp, K. A.; Wang, L.-P.; Simmonett, A. C.; Harrigan, M. P.; Stern, C. D.; et al. OpenMM 7: Rapid Development of High Performance Algorithms for Molecular Dynamics. *PLoS Comput. Biol.* **2017**, *13*, No. e1005659.
(116) Case, D.; Cheatham III, T.; Darden, T.; Gohlke, H.; Luo, R.; Merz Jr, K.; Onufriev, A.; Simmerling, C.; Wang, B.; Woods, R. The Amber Biomolecular Simulation Programs. *J. Comput. Chem.* **2005**, *26*, 1668.
(117) Jung, J.; Mori, T.; Kobayashi, C.; Matsunaga, Y.; Yoda, T.; Feig, M.; Sugita, Y. GENESIS: a hybrid-parallel and multi-scale molecular dynamics simulator with enhanced sampling algorithms for biomolecular and cellular simulations. *Wiley Interdisciplinary Reviews: Computational Molecular Science* **2015**, *5*, 310−323.
(118) Tribello, G. A.; Bonomi, M.; Branduardi, D.; Camilloni, C.; Bussi, G. PLUMED 2: New Feathers for an Old Bird. *Comput. Phys. Commun.* **2014**, *185*, 604−613.
(119) Li, J.; Wen, P.-C.; Moradi, M.; Tajkhorshid, E. Computational Characterization of Structural Dynamics Underlying Function in Active Membrane Transporters. *Curr. Opin. Struct. Biol.* **2015**, *31*, 96−105.
(120) Ravindra, P.; Smith, Z.; Tiwary, P. Automatic Mutual Information Noise Omission (AMINO): Generating Order Parameters for Molecular Systems. *Molecular Systems Design & Engineering* **2020**, *5*, 339−348.
(121) Smith, Z.; Ravindra, P.; Wang, Y.; Cooley, R.; Tiwary, P. Discovering Protein Conformational Flexibility Through Artificial-Intelligence-Aided Molecular Dynamics. *J. Chem. Phys.* **2020**, *124*, 8221−8229.
(122) Pant, S.; Smith, Z.; Wang, Y.; Tajkhorshid, E.; Tiwary, P. Confronting Pitfalls of AI-augmented Molecular Dynamics Using Statistical Physics. *J. Chem. Phys.* **2020**, *153*, 234118 DOI: 10.1063/5.0030931.
(123) Mehdi, S.; Wang, D.; Pant, S.; Tiwary, P. Accelerating All-atom Simulations and Gaining Mechanistic Understanding of Biophysical Systems Through State Predictive Information Bottleneck. *J. Chem. Theory Comput.* **2022**, *18*, 3231−3238.

(124) Oh, M.; Rosa, M.; Xie, H.; Khelashvili, G. Automated Collective Variable Discovery for MFSD2A Transporter From Molecular Dynamics Simulations. *Biophys. J.* **2024**, *123*, 2934−2955.
(125) Schlessinger, A.; Bonomi, M. Exploring the Conformational Diversity of Proteins. *eLife* **2022**, *11*, No. e78549.
(126) Thangapandian, S.; Fakharzadeh, A.; Moradi, M.; Tajkhorshid, E. Conformational free energy landscape of a glutamate transporter and microscopic details of its transport mechanism. *Proc. Natl. Acad. Sci. U.S.A.* **2025**, *122* (10), No. e2416381122.
(127) Martens, C.; Shekhar, M.; Borysik, A.; Lau, A.; Reading, E.; Tajkhorshid, E.; Booth, P. J.; Politis, A. Direct Protein-lipid Interactions Shape the Conformational Landscape of Secondary Transporters. *Nat. Commun.* **2018**, *9*, 4151.
(128) Rasouli, A.; Yu, Q.; Dehghani-Ghahnaviyeh, S.; Wen, P.-C.; Kowal, J.; Locher, K. P.; Tajkhorshid, E. Differential Dynamics and Direct Interaction of Bound Ligands with Lipids in Multidrug Transporter ABCG2. *Proc. Natl. Acad. Sci. U.S.A.* **2023**, *120*, No. e2213437120.
(129) Tang, Q.; Sinclair, M.; Hasdemir, H. S.; Stein, R. A.; Karakas, E.; Tajkhorshid, E.; Mchaourab, H. S. Asymmetric Conformations and Lipid Interactions Shape the ATP-coupled Cycle of a Heterodimeric ABC Transporter. *Nat. Commun.* **2023**, *14*, 7183.
(130) Sinclair, M.; Stein, R. A.; Sheehan, J. H.; Hawes, E. M.; O'Brien, R. M.; Tajkhorshid, E.; Claxton, D. P. Integrative Analysis of Pathogenic Variants in Glucose-6-phosphatase Based on an AlphaFold2 Model. *PNAS Nexus* **2024**, *3*, pgae036.
(131) Kapoor, K.; Pant, S.; Tajkhorshid, E. Active Participation of Membrane Lipids in Inhibition of Multidrug Transporter P-glycoprotein. *Chem. Sci.* **2021**, *12*, 6293−6306.
(132) Pant, S.; Zhang, J.; Kim, E.; Lam, K.; Chung, H. J.; Tajkhorshid, E. PIP2-dependent Coupling of Voltage Sensor and Pore Domains in Kv7.2. *Commun. Biol.* **2021**, *4*. DOI: 10.1038/s42003-021-02729-3
(133) Crespi, V.; Tóth, Á.; Janaszkiewicz, A.; Falguières, T.; Di Meo, F. Membrane-Dependent Dynamics and Dual Translocation Mechanisms of ABCB4: Insights from Molecular Dynamics Simulations. *bioRxiv* **2024**, 2024−10.
(134) Tóth, Á.; Janaszkiewicz, A.; Crespi, V.; Di Meo, F. On the Interplay Between Lipids and Asymmetric Dynamics of an NBS Degenerate ABC Transporter. *Commun. Biol.* **2023**, *6*, 149.
(135) Janaszkiewicz, A.; Tóth, Á.; Faucher, Q.; Martin, M.; Chantemargue, B.; Barin-Le Guellec, C.; Marquet, P.; Di Meo, F. Insights into the structure and function of the human organic anion transporter 1 in lipid bilayer membranes. *Sci. Rep.* **2022**, *12*, 7057.
(136) Le, L. T. M.; Thompson, J. R.; Dehghani-Ghahnaviyeh, S.; Pant, S.; Dang, P. X.; French, J. B.; Kanikeyo, T.; Tajkhorshid, E.; Alam, A. Cryo-EM Structures of Human ABCA7 Provide Insights into its Phospholipid Translocation Mechanisms. *EMBO J.* **2023**, *42*, No. e111065.
(137) Martens, C.; Shekhar, M.; Lau, A. M.; Tajkhorshid, E.; Politis, A. Integrating Hydrogen-Deuterium Exchange Mass Spectrometry with Molecular Dynamics Simulations to Probe Lipid-modulated Conformational Changes in Membrane Proteins. *Nat. Protocols* **2019**, *14*, 3183−3204.
(138) Zhang, Y.; Soubias, O.; Pant, S.; Heinrich, F.; Vogel, A.; Li, J.; Li, Y.; Clifton, L. A.; Daum, S.; Bacia, K.; et al. Myr-Arf1 conformational flexibility at the membrane surface sheds light on the interactions with ArfGAP ASAP1. *Nat. Commun.* **2023**, *14* (1), 7570.
(139) Muñoz, K. A.; Vasan, A. K.; Sinclair, M.; Wen, P.-C.; Holmes, J. R.; Ulrich, R. J.; Lee, H. Y.; Hung, C.-C.; Fields, C. J.; Tajkhorshid, E.; et al. A Gram-negative-selective Antibiotic Spares the Gut Microbiome and Prevents *Clostridioides Difficile* Infection. *Nature* **2024**, *630*, 429−436.
(140) Del Alamo, D.; Sala, D.; Mchaourab, H. S.; Meiler, J. Sampling alternative conformational states of transporters and receptors with AlphaFold2. *eLife* **2022**, *11*, No. e75751.
(141) Kapoor, K.; Thangapandian, S.; Tajkhorshid, E. Extended-Ensemble Docking to Probe Dynamic Variation of Ligand Binding Sites During Large-Scale Structural Changes of Proteins. *Chem. Sci.* **2022**, *13*, 4150−4169.
(142) Tu, G.; Xu, B.; Luo, D.; Liu, J.; Liu, Z.; Chen, G.; Xue, W. Multi-state Model-Based Identification of Cryptic Allosteric Sites on Human Serotonin Transporter. *ACS Chem. Neurosci.* **2023**, *14*, 1686−1694.
(143) Shi, S.; Ma, B.; Ji, Q.; Guo, S.; An, H.; Ye, S. Identification of a Druggable Pocket of the Calcium-activated Chloride Channel TMEM16A in Its Open State. *J. Biol. Chem.* **2023**, *299*, 104780.

https://doi.org/10.1021/acs.jpcb.5c00104
J. Phys. Chem. B 2025, 129, 3703−3719